The Mesoproterozoic Basement at the San Rafael Block, Mendoza Province (Argentina): Geochemical and Isotopic Age Constraints

Carlos A. Cingolani, Miguel A.S. Basei, Ricardo Varela, Eduardo Jorge Llambías, Farid Chemale Jr., Paulina Abre, Norberto Javier Uriz and Juliana Marques

Abstract This work provides new petro-geochemical and isotopic information to constrain the crustal evolution of the Precambrian Cerro La Ventana Formation. The Rb–Sr, Sm–Nd, Pb–Pb, and U–Pb isotopic data obtained as well as their

Electronic supplementary material The online version of this chapter (doi:10.1007/978-3-319-50153-6_2) contains supplementary material, which is available to authorized users.

C.A. Cingolani (✉) · R. Varela · E.J. Llambías
Centro de Investigaciones Geológicas-CONICET, Universidad Nacional de La Plata, Diag. 113 n. 275, 1904 La Plata, Argentina
e-mail: ccingola@cig.museo.unlp.edu.ar; carloscingolani@yahoo.com

R. Varela
e-mail: ricardovarela4747@gmail.com

E.J. Llambías
e-mail: llambias@cig.museo.unlp.edu.ar

M.A.S. Basei
Centro de Pesquisas Geocronológicas (CPGeo), Universidade de São Paulo, Instituto de Geociencias, São Paulo, Brazil
e-mail: baseimas@usp.br

F. Chemale Jr.
Programa de Pós-Graduação em Geologia, Universidade do Vale do Rio dos Sinos (UNISINOS), 93022-000 São Leopoldo, Brazil
e-mail: faridchemale@gmail.com

P. Abre
CURE-UDELAR Ruta 8 Km 282, 33000 Treinta y Tres, Uruguay
e-mail: pabre@cure.edu.uy

C.A. Cingolani · N.J. Uriz
División Geología del Museo de La Plata, Paseo del Bosque S/N, 1900 La Plata, Argentina
e-mail: norjuz@gmail.com

J. Marques
Laboratorio de Geologia Isotópica, Universidade Federal do Río Grande do Sul, Porto

© Springer International Publishing AG 2017

C.A. Cingolani (ed.), *Pre-Carboniferous Evolution of the San Rafael Block, Argentina*, Springer Earth System Sciences,
DOI 10.1007/978-3-319-50153-6_2

petrological and geochemical features are reported. These data are useful to discuss relationships with equivalent Mesoproterozoic units located along the Cuyania terrane in the proto-Andean Gondwana margin. The type section of the basement rocks of the Cerro La Ventana Formation is located in the south-eastern part of the San Rafael Block, Mendoza Province known as Leones-Ponón Trehué-La Estrechura region. Equivalent crustal fragments are also included in this basement, such as ductile-deformed rocks of the El Nihuil Mafic Unit that are intruded by Ordovician undeformed dolerites. The basement exposed along the type section corresponds to a metamorphosed volcano-plutonic complex with hardly any sedimentary protolith. Main rocks are tonalites and foliated gabbros and quartz diorites that pass to amphibolites, and minor granodioritic–dioritic orthogneisses, with abundant angular microgranitoid enclaves now deformed and stretched intruded in mafic to felsic metavolcanics with porphyritic relic textures. The studied samples classified as tonalites and some close to the field of granodiorites following a calc-alkaline trend. Gabbroic samples from the El Nihuil mafic unit show a more tholeiitic signature. The bulk of samples from the Cerro La Ventana Formation plot within the field of metaluminous rocks; although a few are in the peraluminous field. Main groups of samples plot as low-Al TTD field; however, some of them show high Sr/Y ratios which are typical of high-Al TTD. The Mg#/K ratio is higher in the Cerro La Ventana Formation compared with Las Matras TTG series suggesting a minor differentiated grade for the first one. The chondrite-normalized REE diagrams for Leones samples have Eu anomalies rather positive and gabbros from El Nihuil region display patterns with positive Eu anomalies typical of plagioclase-rich igneous rocks. The Rb–Sr data defined an isochron with 1148 ± 83 Ma, initial $^{87}Sr/^{86}Sr = 0.70292 \pm 0.00018$. The low initial ratio is indicative of a slight evolved Mesoproterozoic source. An acceptable isochron was obtained using Sm–Nd methodology indicating an age of 1228 ± 63 Ma. The model ages (T_{DM}) are in the range 1.23–1.64 Ga with $\varepsilon Nd_{(1200)}$ in between −0.94 and +4.7 recording a 'depleted' source, less evolved than CHUR for the time of crystallization. In a $^{207}Pb/^{204}Pb$ diagram the samples plot similarly to rocks from the basement of Cuyania Terrane (Pie de Palo Range and crustal xenoliths) showing a distinctive non-radiogenic signature. The tonalitic lithofacies located at the Leones River type section was chosen for zircon U–Pb TIMS dating and the obtained crystallization age was 1214.7 ± 6.5 Ma. The in situ U–Pb (LA-ICP-MS) zircon data done in two different laboratories on samples from El Nihuil mafic unit (tonalitic orthogneisses) plotted in a Concordia diagram, record an intercept at 1256 ± 10 Ma and in Tera-Wasserburg diagram an age of 1222 ± 6.9 Ma. With these isotopic data we confirm the Mesoproterozoic age for the basement of the San Rafael Block. The obtained *ca*. 1.2 Ga is quite similar to those belonging to the basement of other regions from the Cuyania allochthonous terrane.

Alegre, Brazil
e-mail: juliana.marques@ufrgs.br

Keywords Cuyania terrane · San Rafael Block · Cerro La Ventana Formation · Mesoproterozoic basement · Geochemistry · Geochronology

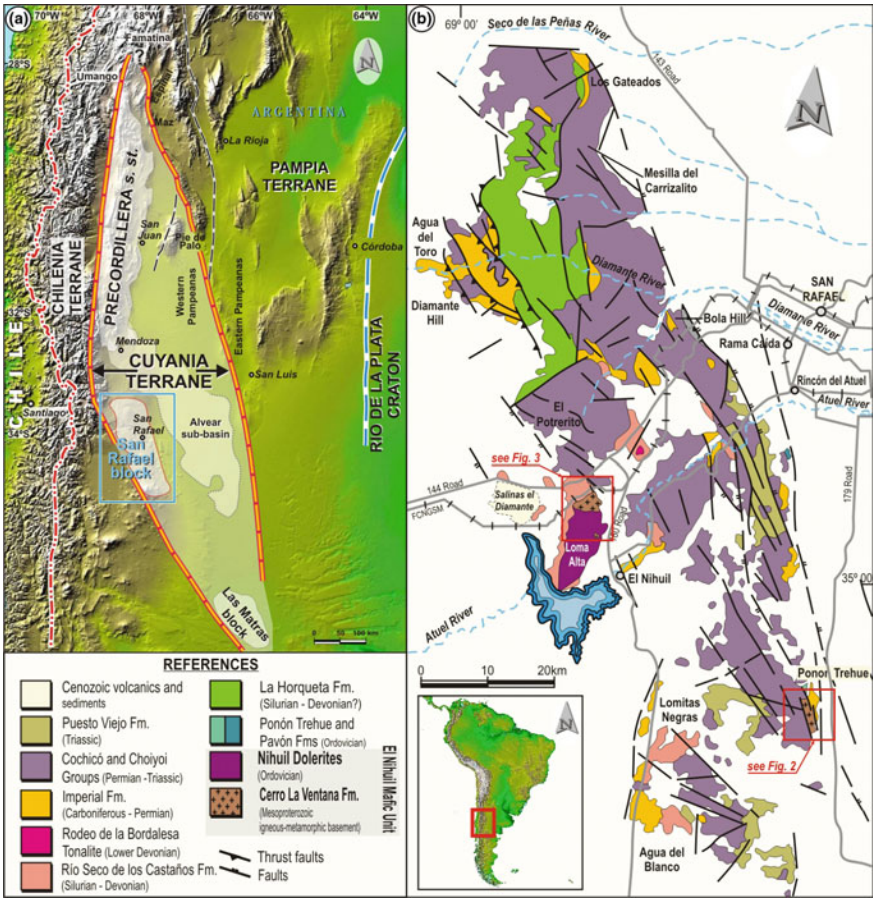

Fig. 1 **a** Location of the San Rafael Block within the Cuyania terrane along the proto-Andean margin of Gondwana; **b** geological sketch map of the San Rafael Block and the position of the studied regions

1 Introduction

The southern South America Paleozoic Gondwana margin (Fig. 1) is characterized by the presence of orogenic belts oriented approximately north-south (Ramos et al. 1986; Dalla Salda et al. 1992). They have been accreted to the cratonic areas during the Cambrian (Pampean), Mid-Ordovician (Famatinian), and Upper Devonian (Gondwanian) tectonic cycles. The Argentine Precordillera or Cuyania composite terrane in the sense of Ramos (2004 and references) is linked to the Famatinian cycle and lies eastward of the present-day Andes. This terrane had been considered from the standpoint of stratigraphy and faunal unique to South America mainly for the Lower Paleozoic carbonate and siliciclastic deposits overlying an igneous–metamorphic crust of Grenville age (Ramos et al. 1998; Sato et al. 2004; Varela et al. 2011). The composite terrane comprises four sectors: The Precordillera (28°–33°S) mainly thin-skinned fold and thrust belt generated by shallow east-dipping flat-slab subduction of the Nazca plate, the Pie de Palo area, and the San Rafael and the Las Matras blocks (Fig. 1).

The San Rafael Block (SRB) lies in west-central Mendoza Province, Argentine (35°S–68° 30′W), and has SSE-NNW structural Cenozoic trend in the pre-Andean region. To the North and South the Cuyo and Neuquén sedimentary basins bound it, respectively. Toward East the outcrops of the SRB vanish under the modern basaltic back arc volcanism and sedimentary cover; the Western boundary is defined by the Andean foothill (Fig. 1). The SRB is interpreted as an extension of the Precordillera region on the light of paleontological and geological evidence (Ramos 1995; Ramos et al. 1999; Keller 1999). Diverse igneous-metamorphic and sedimentary units of Precambrian to Middle Paleozoic age, known as 'pre-Carboniferous units' due to their clear differentiation below a Carboniferous regional unconformity (Dessanti 1956), crop out within the SRB. Basement crustal rocks known as Cerro La Ventana Formation (Criado Roqué 1972) are exposed in the eastern and central part of the SRB (type section: 35° 12′S–68° 17′W), partially covered by calcareous–siliciclastic sedimentary rocks bearing Ordovician macro- and microfossils (Nuñez 1962, 1976; Heredia 2006; Abre et al. 2011; Heredia and Mestre, this volume).

The main purpose of this work is to provide new petro-geochemical and isotopic information to constrain the crustal evolution of the Precambrian Cerro La Ventana Formation. The Rb–Sr, Sm–Nd, Pb–Pb, and U–Pb isotopic data obtained as well as their petrological and geochemical features are reported in this paper. These data are useful to discuss relationships with equivalent Mesoproterozoic units located along the Cuyania terrane in the proto-Andean Gondwana margin.

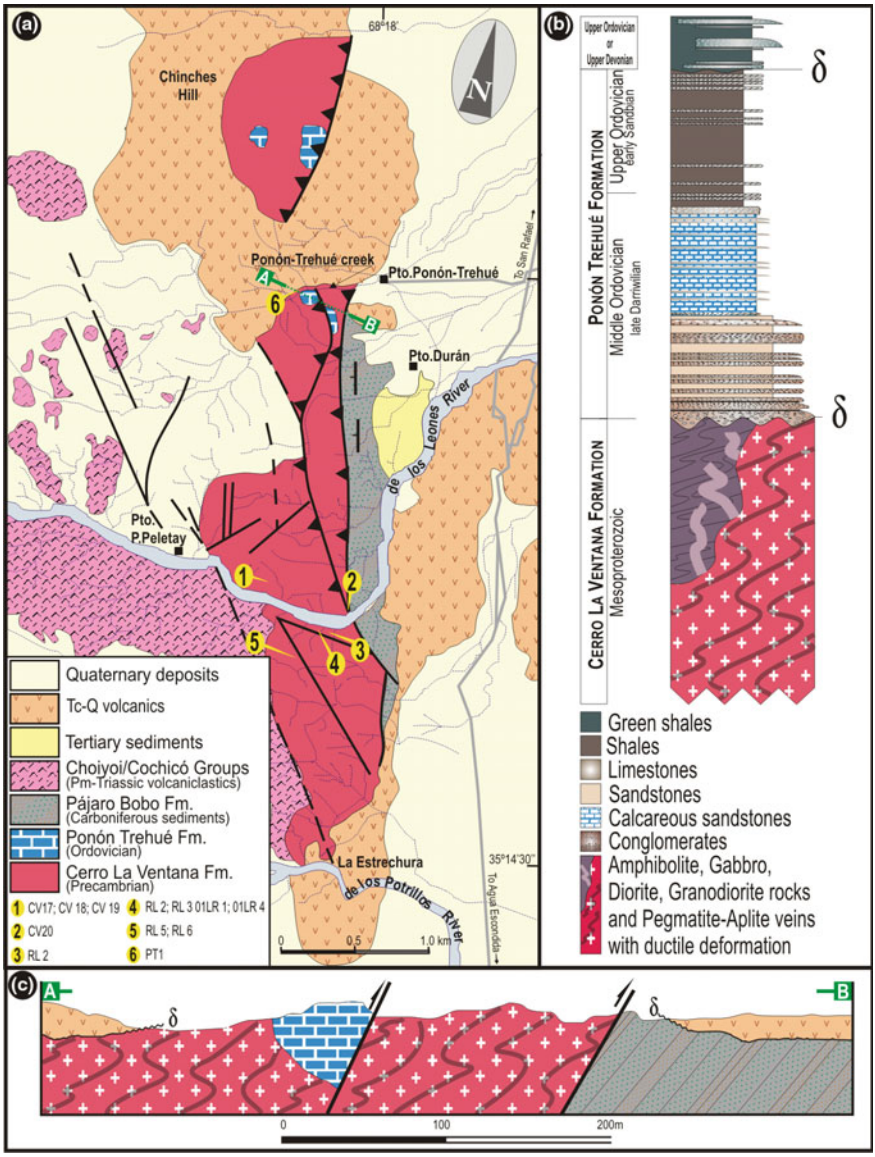

Fig. 2 **a** Geological sketch map from the Leones-Ponón Trehué creeks toward the south up La Estrechura section (based in Nuñez 1979; Bordonaro et al. 1996; Astini 2002; Cingolani et al. 2005). Locations of the samples are in *yellow*. **b** Stratigraphic column showing the Cerro La Ventana basement and unconformity contact with the Ordovician Ponón Trehué Formation (modified from Heredia 2006). **c** Schematic profile at the Ponón Trehué creek showing the tectonic relationships between basement rocks and other units

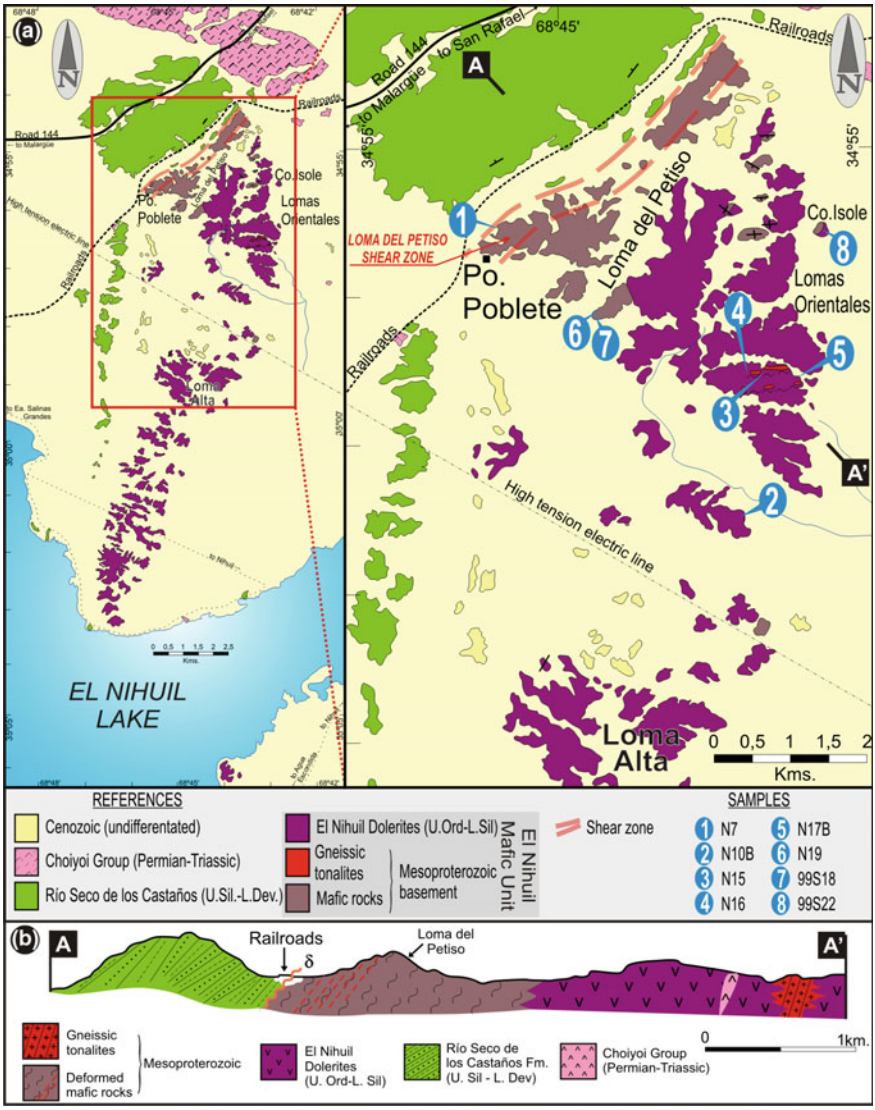

Fig. 3 **a** Geological sketch map of the El Nihuil mafic unit where the Mesoproterozoic basement is exposed (modified from Cingolani et al. 2000). The locations of the studied samples are in *blue*; **b** schematic profile showing the relationships between units

2 Geological Setting

The type section of the basement rocks of the Cerro La Ventana Formation (Criado Roqué 1972) or La Ventana Formation (Nuñez 1979) is located in the south-eastern part of the SRB, Mendoza Province (Fig. 2) known as Leones-Ponón Trehué-La Estrechura region (hereafter 'Leones'), in a NNW-SSE trending belt of about 9 km long and 1.5 km wide. It consists of an igneous–metamorphic complex, acidic to intermediate granitoids, as well as pegmatitic and aplitic veins.

Equivalent crustal fragments are also included in this basement, such as ductile-deformed rocks of the El Nihuil mafic unit outcropping at Lomas Orientales and Loma del Petiso (Fig. 3) intruded by undeformed Ordovician dolerites.

Also we mention the 'basement rocks' that were localized in petroleum research wells (Criado Roqué 1979; Criado Roqué and Ibáñez 1979) toward the southeast ('Alvear sub-basin' at Triassic Cuyo Basin). The Cerro Las Pacas Formation (Holmberg 1973) was previously considered as part of the basement; however, new isotopic data done by Cingolani et al. (2014) on mica schists with vertical foliation and intruded by Permian magmatism, record U–Pb detrital zircon ages as young as *ca*. 376 Ma, and therefore it no longer can be considered as part of the Proterozoic basement of the Cuyania terrane. Oil exploration carried out before 1970 in the underground of Triassic Cuyo Basin, 'basement' rocks correlated with the Cerro La Ventana Formation were recognized to the east of the San Rafael Block, at the Alvear sub-basin (Ramos 2004). The borehole IV-D cut garnet–hornblende–biotite schists that recorded a K–Ar age of 605 Ma (Criado Roqué 1979). Close to Corral de Lorca town the exploration well cut metasedimentary rocks (mica schists) from which Cingolani et al. (2012a) obtained U–Pb detrital zircon ages of 395–410 Ma. These rocks are very different to those from the Mesoproterozoic basement and could be correlated to the La Horqueta Formation (Silurian–Devonian age) instead.

It is important to mention that the Leones type section (Ponón Trehué region) constitutes an interesting study area since it records the primary contact between the basement (Cerro La Ventana Formation) and the Precordilleran Lower Paleozoic platform sedimentary rocks (Fig. 2a, b). After Nuñez (1979), Bordonaro et al. (1996), Heredia (1996), and Astini (2002), the two sedimentary members mapped in the area were genetically related to an episode of extension but deposited in separate areas, although both overlie basement rocks. The first one was interpreted as an accumulation of allochthonous (resedimented) carbonate blocks and olistoliths (limestone and igneous blocks) in the proximal reaches of graben. The second unit comprises a lower section composed of sandy carbonates yielding a well-preserved mid-Ordovician conodont and shelly fauna, and resting unconformably on the basement, while the upper section is siliciclastic in composition. Together they provide a record of extensional history (Astini 2002; Abre et al. 2011 and references).

3 History of the Basement Knowledge

Stappenbeck (1913) in his extensive travel from the Sierra Pintada to Cerro Nevado achieved the first reference on basement rocks, and in the La Estrechura (de los Potrillos River) he mentioned the presence of basement gneisses supposedly brought up to the surface by modern basalts. Wichmann (1928) mentioned basement rocks such as gneisses, granites, pegmatites, amphibolites among others, and limestones (outcropping toward west of the Cenozoic volcano Ponón Trehué Hill), which he considered similar to those of the Cerro de la Cal and Salagasta (near the city of Mendoza). Polanski (1949) named the basement as 'Serie de Ponon-Trehue'. Padula (1949, 1951) mapped the region while working for the oil industry and described granitic orthogneisses supporting Ordovician limestones in unconformity and with tectonic contacts with younger Upper Paleozoic sedimentary and volcanic rocks. Criado Roqué (1972) assigned the igneous–metamorphic complex composed mainly of deformed mafic-amphibolite and granitoid rocks, to the Precambrian and named it as Cerro La Ventana Formation. This unit was correlated based on rock similarities to the Pie de Palo outcrops. The basement along the Seco de los Leones River and Ponón Trehué creek was also referred to as La Ventana Formation by Nuñez (1979). He described the petrographical characteristics of the recognized rocks, affected by heterogeneous ductile shear zones, such as amphibolites, mica schists, metaquartzites, gneisses, amphibolitic schists, granites, diorites, and pegmatitic and aplitic veins. Rolleri and Criado Roqué (1970) and Rolleri and Fernández Garrasino (1979) mentioned the presence of high-metamorphic grade 'Pre-Paleozoic Basement' with amphibolites, gabbros, mica schists, amphibolitic schists, and quartzites, intruded by granites and pegmatite–aplite veins. The authors pointed out the presence of intercalated mafic rocks recording pre-orogenic magmatism similar to the Cerros Valdivia and Barbosa (near San Juan city). This complex supports in unconformity an Ordovician sedimentary cover and its exposures are characterized by compressive features such as tectonic contacts acquired during Cenozoic east-vergence thrusting that juxtaposed the basement rocks with both Ordovician and Upper Paleozoic rocks (Fig. 2b, c). Deformation and associated low-grade metamorphism heterogeneously affected this association, originating discrete belts of gneisses. Caminos (1993) correlated the San Rafael Block Precambrian basement to the Western Pampeanas Ranges. Astini et al. (1996) and Thomas et al. (2012) cited an unpublished U–Pb age that yielded a Grenvillian age for the basement rocks. Davicino and Sabalúa (1990) report geochemistry information on mafic rocks and described mylonite and cataclastic rocks along the El Nihuil mafic unit. First Rb–Sr data were obtained by Cingolani and Varela (1999) from seven samples of granodioritic to tonalitic rocks, exposed along the Seco de los Leones and Ponón Trehué creeks; their whole-rock isochron yielded a Mesoproterozoic age of 1063 ± 106 Ma. For more detailed references see also Sato et al. (2000, 2004), Casquet et al. (2006), Vujovich et al. (2004), Ramos (2004), Rapela et al. (2010), and Cingolani et al. (2000, 2012b, 2014). A comprehensive review of the geological and isotopic features of Grenvillian-age

Table 1 GPS coordinates of the studied samples at different outcrop sectors

Sample	GPS	Rock type	Methodology
Leones type section			
CV17	35° 12′ 26″S–68° 18′ 32″W	Tonalite	Pb/Pb; Sm/Nd; geochemistry
CV18	35° 12′ 26″S–68° 18′ 32″W	Gabbro–diorite	Pb/Pb; Sm/Nd; geochemistry
CV19	35° 12′ 26″S–68° 18′ 32″W	Gabbro–diorite (Biot.–Qz)	Pb/Pb; Sm/Nd; geochemistry
CV20	35° 12′ 23″S–68° 17′ 33″W	Deformed tonalite (garnet)	Pb/Pb; Sm/Nd; geochemistry
RL2	35° 12′ 39″S–68° 17′ 53″W	Granitic composition	Rb/Sr
RL3	35° 12′ 40″S–68° 18′ 06″W	Granitic composition	Geochemistry; Rb/Sr
RL4	35° 12′ 40″S–68° 18′ 06″W	Granitic composition	Geochemistry; Rb/Sr
RL5	35° 12′ 53″S–68° 18′ 19″W	Granitic composition	Rb/Sr
RL6	35° 12′ 53″S–68° 18′ 19″W	Tonalite	Geochemistry; Rb/Sr
01RL1	35° 12′ 36″S–68° 17′ 38″W	Gabbro	Geochemistry
01RL2	35° 12′ 36″S–68° 17′ 48″W	Dioritic composition	U–Pb
01RL3	35° 12′ 33″S–68° 18′ 14″W	Granitic composition	U–Pb
01RL4	35° 12′ 33″S–68° 18′ 14″W	Granitic composition	Geochemistry
01RL5	35° 12′ 33″S–68° 18′ 14″W	Dioritic composition	Geochemistry
PT1	35° 10′ 01″S–68° 18′ 53″W	Granitic composition	Rb/Sr
El Nihuil mafic unit			
N7	34° 55′ 35.6″S–68° 45′ 21.6″W	Gabbro	Geochemistry; Rb/Sr
N10B	34° 57′ 37.4″S–68° 43′ 28.1″W	Gabbro	Geochemistry
N19	34° 56′ 07.8″S–68° 44′ 33.7″W	Foliated gabbro	Geochemistry; Rb/Sr
N15	34° 56′ 39.7″S–68° 43′ 18.8″W	Foliated tonalite-granodiorite	Sm/Nd; U–Pb; geochemistry
N16	34° 56′ 36.4″S–68° 43′ 13.7″W	Granitic composition	Geochemistry
N17B	34° 56′ 37.8″S–68° 43′ 04.5″W	Granitic composition	U–Pb; geochemistry
99S22	34° 55′ 40.8″S–68° 42′ 44.0″W	Gabbro	Rb/Sr
99S18	34° 55′ 38.5″S–68° 45′ 25.6″W	Gabbro	Rb/Sr

rocks attached to the southwest of the Río de la Plata craton in Early Paleozoic times was presented by Varela et al. (2011). In this paper, the Mesoproterozoic basement exposures are clearly extended southward of 34°S in the Cuyania terrane, specifically within de San Rafael and Las Matras blocks (Fig. 1). The main difference is the pervasive foliation and subsequent mylonitization that affect the Cerro La Ventana Formation in the San Rafael Block. In this scenario the shallower crustal level is exposed toward the South (Las Matras) as a Grenvillian-age tonalitic-trondhjemitic pluton.

Table 2 Analytical results of major (in w/%) and trace elements (in ppm) in the studied samples (ACTLABS, Canada)

Samples	Leones type section								El Nihuil mafic unit					
	RL3	RL4	RL6	01RL1	01RL2	01RL3	01RL4	01RL5	N7	N10B	N19	N15	N16	N17B
Major elements														
SiO_2	72.65	71.03	68.57	70.92	53.71	55.76	55.37	56.26	48.63	43.24	51.17	65.94	66.04	65.80
Al_2O_3	14.51	14.05	15.12	14.11	16.31	17.96	16.63	15.70	16.01	19.94	23.4	15.06	15.03	15.13
Fe_2O_3	1.62	2.90	3.10	3.64	8.45	7.62	7.91	8.55	9.93	11.74	5.42	4.45	4.14	4.29
MnO	0.02	0.042	0.063	0.07	0.15	0.109	0.125	0.12	0.177	0.127	0.064	0.06	0.07	0.07
MgO	0.50	0.91	1.11	0.79	5.08	3.56	4.11	3.09	6.71	4.34	1.63	2.08	2.11	2.08
CaO	3.25	2.99	3.50	3.65	8.47	7.40	7.08	5.86	10.1	11.3	10.78	4.62	5.22	4.40
Na_2O	4.38	4.18	3.94	3.90	3.61	3.60	3.69	4.02	2.98	2.55	3.76	5.14	3.55	3.68
K_2O	0.90	1.09	1.85	0.81	1.39	1.05	1.37	2.23	0.33	0.56	0.86	0.43	1.23	1.92
TiO_2	0.186	0.341	0.326	0.25	0.52	0.888	0.94	1.29	1.22	2.03	0.71	0.44	0.44	0.45
P_2O_5	0.06	0.12	0.12	0.06	0.11	0.24	0.34	0.47	0.05	0.82	0.12	0.18	0.17	0.18
LOI	1.04	1.35	1.28	1.80	2.20	2.28	2.10	2.40	3.73	2.95	2.54	2.08	2.17	2.14
Total	99.13	99.01	98.98	0.00	0.00	100.46	99.64	99.99	99.86	99.6	100.48	100.49	100.17	100.13
Al_2O_3/SiO_2	0.20	0.20	0.22	0.20	0.30	0.32	0.30	0.28	0.33	0.46	0.46	0.23	0.23	0.23
K_2O/Na_2O	0.21	0.26	0.47	0.21	0.39	0.29	0.37	0.55	0.11	0.22	0.23	0.08	0.35	0.52
Mg#*100	55	55	59	46	70	65	67	59	73	59	54	65	67	66
Trace elements														
Sc	2	3	10			16	18							
V	15	33	43			131	128							
Cr	36	23	34			20	86							
Co	37	33	27			31	34							
Ni	−20	−20	−20			30	75							
Cu	−10	14	15			75	47							

(continued)

Table 2 (continued)

Samples	Leones type section								El Nihuil mafic unit					
	RL3	RL4	RL6	01RL1	01RL2	01RL3	01RL4	01RL5	N7	N10B	N19	N15	N16	N17B
Zn	−30	57	49			79	94							
Ga	14	15	17			18	18		17	19	21	16	16	15
Ge	1.1	0.8	0.9			1.0	1.1							
Rb	13	18	34			17	26		3	13	20	10	23	34
Sr	445	461	407	252.00	370.00	666	482	420.00	588	668	747	378	392	460
Y	2.4	5.1	12.4	12.00	14.00	12.3	18.5	28.00	10.50	14.70	8.90	15.50	15.90	14.20
Zr	75	145	99	75.00	36.00	29	104	193.00	14	23	33	114	114	104
Nb	1.8	2.9	4.6	1.00	0.00	2.4	11.0	9.00	1.00	2.20	2.00	7.3	7.5	6.7
Cs	0.2	0.2	1.0			0.4	0.2		0.4	0.9	0.3	0.70	0.70	1.60
Ba	805	863	918			519	517		398	326	323	397	1160	1400
Hf	1.9	3.9	2.7	3.40	3.60	1.0	2.7	3.20	0.50	0.70	1.00	3.40	3.60	3.20
Ta	2.48	2.09	1.66			0.85	3.51		0.20	0.20	0.70	2.1	3	1.6
Tl	0.08	0.08	0.12			0.11	0.14		0.09	0.11	0.09	0.06	0.13	0.08
Pb	11	8	7			5	5		19	9	9	12	19	6
Th	3.15	6.31	3.25			0.63	1.18		0.12	0.47	0.57	27.08	18.6	15.2
U	0.29	0.60	0.63			0.31	0.71		0.10	0.22	0.26	5.25	4.97	4.49

Table 3 Analytical results obtained by FRX methodology at the University of Río Grande do Sul, Porto Alegre, Brazil

Samples	CV5	CV17	CV18	CV19	CV20
(**a**)					
SiO_2	56.67	69.86	52.83	50.98	72.11
Al_2O_3	16.27	15.34	17.68	16.72	14.22
Fe_2O_3	6.77	3.28	8.06	7.88	3.93
MnO	0.11	0.05	0.12	0.11	0.07
MgO	3.55	1.13	4.64	6.47	0.66
CaO	6.20	4.19	7.62	6.81	3.77
Na_2O	3.62	3.45	3.09	2.74	3.81
K_2O	2.14	0.88	1.76	0.81	0.14
TiO_2	1.00	0.38	1.04	1.27	0.38
P_2O_5	0.22	0.11	0.22	0.28	0.09
LOI	2.50	1.01	1.98	4.96	0.46
Σ	99.05	99.70	99.04	99.03	99.64
Al_2O_3/SiO_2	0.29	0.22	0.33	0.33	0.20
K_2O/Na_2O	0.59	0.26	0.57	0.30	0.04
Fe_2O_3/MgO	1.91	2.90	1.74	1.22	5.95
(**b**)					
Cr	25	37	52	195	18
Co	50	bdl	47	46	6
Ni	39	3	28	89	10
Ga	30	15	21	22	16
Rb	96	8	39	bdl	bdl
Sr	963	735	647	656	275
Y	43	4	21	19	20
Zr	139	196	82	121	135
Nb	7	1	4	7	5
Ba	1026	718	794	398	369
Pb	11	9	8	8	6

bdl below detection limit

4 Sampling and Analytical Techniques

The Cerro La Ventana Formation was sampled at the type section (CV17 to CV20, RL2 to RL-6, 01RL1, 01RL4, PT1), along the Ponón Trehué and Leones creeks (simplified as 'Leones'). Another locality was the El Nihuil mafic unit, ductile-deformed rocks within the Loma del Petiso and Lomas Orientales were sampled (N7, N10B, N19, N15, N16, N17 B). Table 1 summarizes the sampling locations and analytical methodologies applied to each sample.

For petrographic studies we use more than 30 samples from different localities covering the whole type basement rocks. Twelve whole-rock samples were analyzed for major, trace, and REE (Table 2) at ACTLABS Canada, by Fusion-ICP and Fusion-ICP MS, except for major and trace elements of four whole-rock samples (CV17 to CV20) that were analyzed by X-ray fluorescence at the Universidade Federal do Rio Grande do Sul, Porto Alegre, Brazil (Table 3). For the **Rb–Sr** systematic, the Rb and Sr concentrations were acquired by XRF and the isotopic composition on natural Sr by mass spectrometry. The sample preparation, chemical attacks, and Sr concentration with cation exchange resin were carried out in the clean laboratory of the Centro de Investigaciones Geológicas (CIG, University of La Plata, Argentina) while FRX and mass spectrometry were done at the Centro de Pesquisas Geocronológicas (CPGeo), São Paulo, Brazil (Cingolani and Varela 1999). Results were plotted on isochron diagram, using the Isoplot model after Ludwig (2001). The technical procedure for **Sm–Nd** methodology performed at the Laboratorio de Geología Isotópica, Universidade Federal do Rio Grande do Sul, Porto Alegre, Brazil started with rock powders spiked with mixed ^{149}Sm–^{150}Nd spike and dissolved using an HF–HNO_3 mixture and 6 N HCl in Teflon vials, warmed in hot plate until complete dissolution. The REE were extracted using HDEHP-coated Teflon powder. Isotopic compositions were measured with a VG Sector multicollector mass spectrometer. Sm was loaded on Ta filament and Nd on external Ta triple filament (Ta–Re–Ta) with 0.25 N H_3PO_4. All analyses are adjusted for variations instrumental bias due to periodic adjustment of collector positions as monitored by measurements of the internal standard; on this basis the analyses of La Jolla Nd average are 0.511859 ± 0.000010. During the course of the analyses Nd and Sm blanks were lesser than 750 and 150 pg, respectively. **Pb–Pb** isotopic analyses were performed at Laboratorio de Geologia Isotópica, Universidade Federal do Río Grande do Sul, Porto Alegre, Brazil; whole-rock samples were completely dissolved in Teflon vial using an HF–HNO_3 mixture and 6-N HCl. Ion exchange techniques allowed Pb extraction using AG-1 X 8, 200–400 mesh, anion resin. Each sample was dried to a solid and added a solution of HNO_3 with 50 ppb Tl in order to correct the Pb fractionation during the analyses (Tanimizu and Ishikawa 2006). Pb isotopic compositions were measured with a Neptune MC-ICP-MS in static mode, with collecting of 60 ratios of Pb isotopes. The obtained values of NBS 981 common Pb standard during the analyses were in agreement with the NIST values. **U–Pb (ID-TIMS)** procedure of zircon analyses at Centro de Pesquisas Geocronológicas—IGcUSP, Brazil, is as follows: after 10 kg of sample was crushed and reduced to 140–200-mesh grain sizes the portion rich in heavy minerals was treated with bromoform (d = 2.89 g/cm^3) and methyl iodide (d = 3.3 g/cm^3), and the fraction containing the heavy minerals was processed in the Frantz separator at 1.5 A, and split into several zircon-rich no-magnetic fractions. The final purification of each fraction was achieved by hand picking. Each analyzed fraction represents 30 mg of zircon. Dissolution of zircon crystals was carried out with HF and HNO_3 in Teflon micro-bombs in which a mixed $^{205}Pb/^{235}U$ spike was added. A set of 15 micro-bombs arranged in a metal

jacket is left for 3 days in a stove at 200 °C. Then, the HF is evaporated and HCl (6N) added to the micro-bombs, replaced in the stove for 24 h. After the evaporation of HCl 6N, the residue is dissolved in HCl (3N). U and Pb are concentrated and purified by passing the solution in an anionic exchange resin column following the technical procedure after Krogh (1973). The solution enriched in U and Pb is, after addition of phosphoric acid, evaporated until the formation of a micro-drop. The sample is deposited in a rhenium filament and the isotopic composition is determined with multicollector Finnigan MAT 262 solid source mass spectrometer (TIMS). After reduction of the data (PBDAT), the results are plotted in appropriate concordia diagrams using the software ISOPLOT/EX (Ludwig 1999, 2001). During the period of analyses the standard $^{207}Pb/^{206}Pb$ ratios were NBS 983 0.071212 ± 0.00008; NBS 981 0.911479 ± 0.01; and NBS 0.46692 ± 0.01 (Sato and Kawashita 2002). **U–Pb** ages by **LA-ICP-MS** were obtained at Centro de Pesquisas Geocronológicas, São Paulo (N15-N17B), and at Laboratorio de Geología Isotópica, Universidade Federal do Rio Grande do Sul, Porto Alegre (N15), both located in Brazil. Crystal zircons were obtained after crushing and sieving about 3–5 kg of each sample. The fractions retained in less than 140 μm mesh were separated using hydraulic processes to obtain heavy mineral pre-concentrates. These were treated with bromoform to obtain the complete heavy mineral spectra. Methylene iodide was used to achieve a fraction enriched in zircons, followed by an electromagnetic separation with Frantz Isodynamic equipment when necessary. The final selection of crystals, mounted in 2-cm-diameter epoxy resin and polished, was examined under a binocular microscope. The grains were photographed in reflected and transmitted light, and cathodoluminescense (CL) images were produced in order to investigate the internal structures of the zircon crystals as well as to characterize different populations. Choice of spot sites was guided by CL imaging. The U–Pb isotope analyses in both laboratories were performed on zircon grains using a Thermo-Fisher Neptune laser-ablation multicollector inductively coupled plasma mass spectrometer equipped with a 193 Photon laser system. For the operating conditions and instrument settings of the NEPTUNE instrument and laser-ablation system during analytical sessions see Sato et al. (2009) and Bühn et al. (2009), for CPGeo-USP and LGI-UFRGS, respectively. The data are portrayed in Concordia or Tera–Wasserburg diagrams generated with Isoplot/Ex (Ludwig 2001, 2003). U–Pb (LA-ICP-MS) zircon isotopic data are shown in Tables 9 and 10 (in Electronic Supplementary Material).

5 Petrological and Structural Signatures

The studied samples located at the **Leones** type section (Figs. 2 and 4a–g) are classified as basic to mesosilicic gneisses, foliated gabbros, quartz diorites, and tonalites, partially grading to amphibolites and migmatites. This complex is intruded by diorites with structural lineament N10°E/55°SE which yielded migmatite xenoliths.

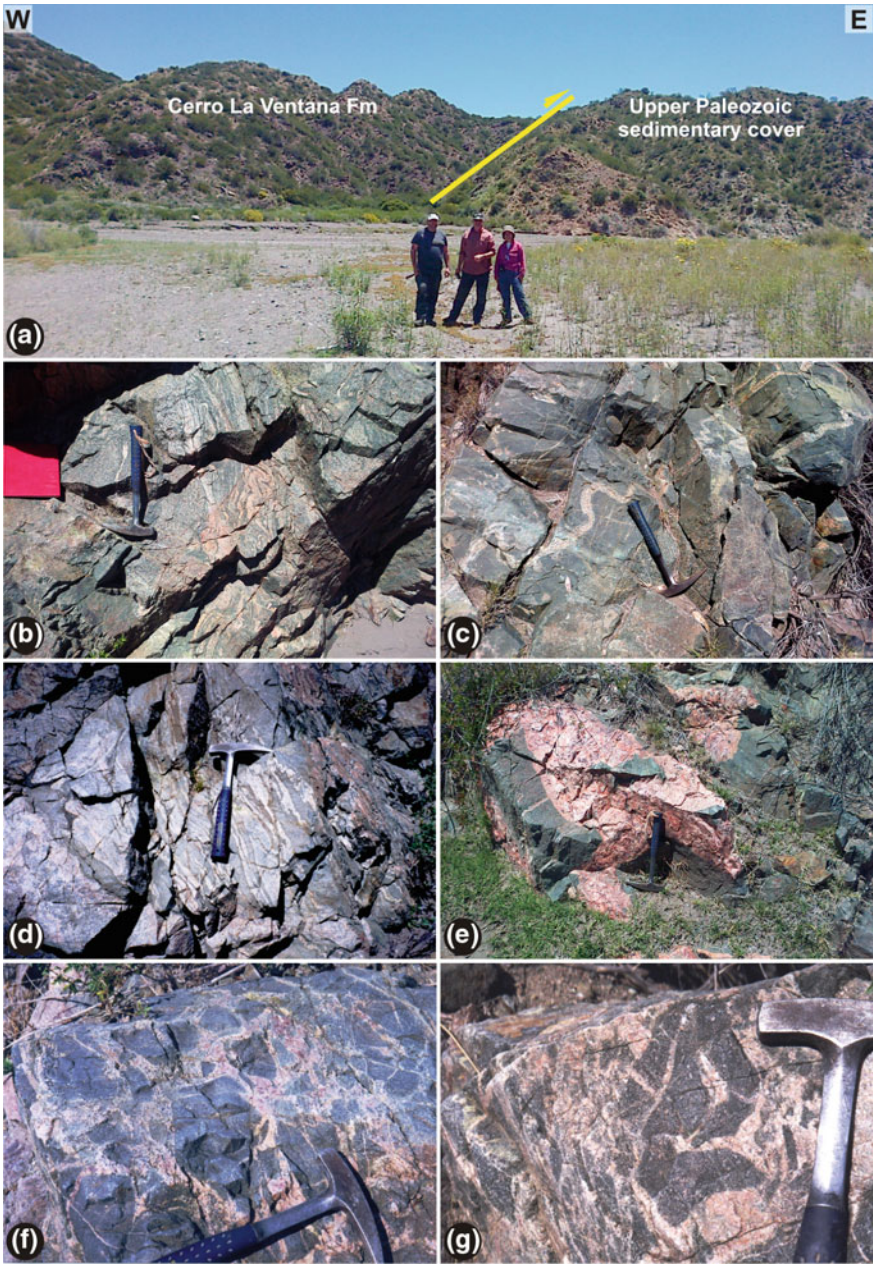

Fig. 4 Field photographs showing the outcrops of Cerro La Ventana Formation at the Leones type section. **a** Thrust fault with east vergence over the Upper Paleozoic unit; **b–d** quartz diorites and tonalites, partially graded to amphibolites; **e** pegmatite veins; **f**, **g** angular dioritic enclaves with textural similarity to Las Matras pluton (Varela et al. 2011)

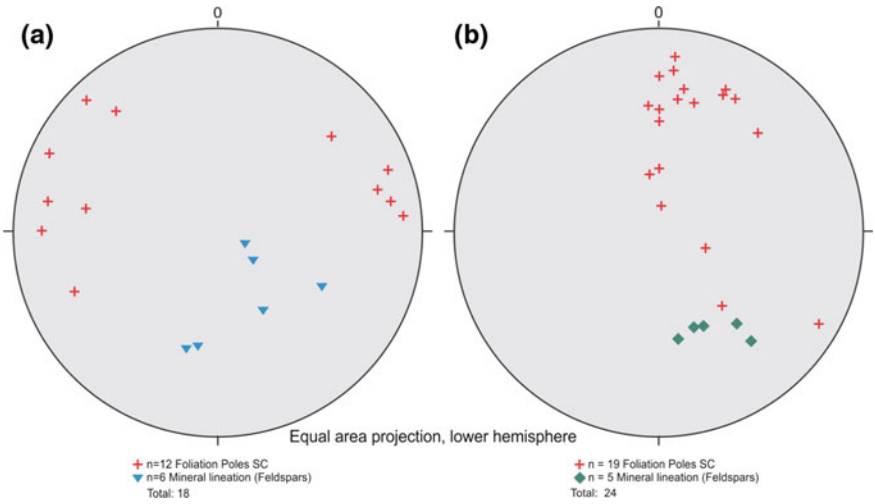

Fig. 5 Measurements of foliation and mineral lineation. **a** Leones type section; **b** El Nihuil mafic unit (tonalitic orthogneisses)

The foliation of some diorites is N20°E/60°NW without any evidence of migmatization. In several places the mentioned rocks are cut by less-deformed pink-granitoids and pegmatites (Fig. 4e). Associated to a vertical faulting with N80°W direction an intense epidotization is present. A ductile deformation is developed with *ca*. N-S shear metamorphic foliation, dipping with high angle toward NW or NE. Linked to the foliation stretching feldspar mineral lineation could be observed, dipping to S or SE. In Fig. 5a, b the structural attitudes of the mylonitic foliation and the mineral lineation are shown, with a main concentration toward N13°W/72°SW. The location of mineral lineation suggests a main transport associated to a shear zone that generated both structures with an important oblique component.

The basement exposed along the type section (Leones River) corresponds to a metamorphosed volcano-plutonic complex with hardly any sedimentary protolith. Main rocks are tonalites and foliated quartz diorites and gabbros that pass to amphibolites, and minor granodioritic–dioritic orthogneisses, with abundant angular microgranitoid enclaves now deformed and stretched (Fig. 4f, g.) intruded in mafic to felsic metavolcanics with porphyritic relic textures. Tabular mafic to felsic dykes cut the country rocks and intrusives and are metamorphosed along with them. In some places from Leones River section the tonalites are rich in garnets (i.e., sample CV20) suggesting that the volcano-plutonic complex could reach the high greenschist–amphibolite facies. Deformation coeval with the metamorphism record the folding of the complex and generated a penetrative foliation S_{x-1} NW-SE dipping 50° to NE and SW. Fold axes have N-S orientation dipping *ca*. 60°S. The foliated quartz-dioritic rocks are composed of less-zoned plagioclase (An_{42}), amphibole, and scarce quartz. Apatite and sphene are most common accessory

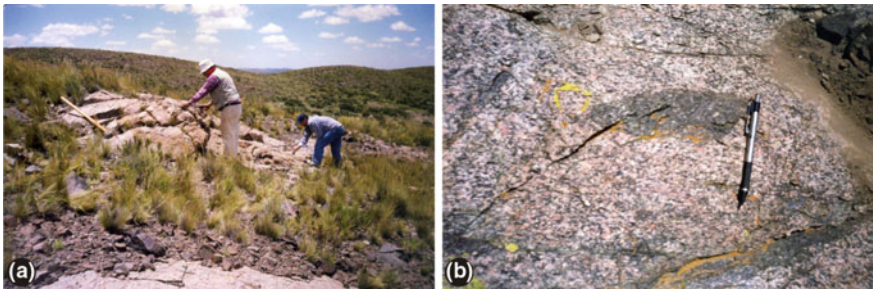

Fig. 6 **a** Lomas Orientales basement outcrops along the El Nihuil mafic unit; **b** studied samples were taken on tonalitic orthogneisses with mafic enclaves

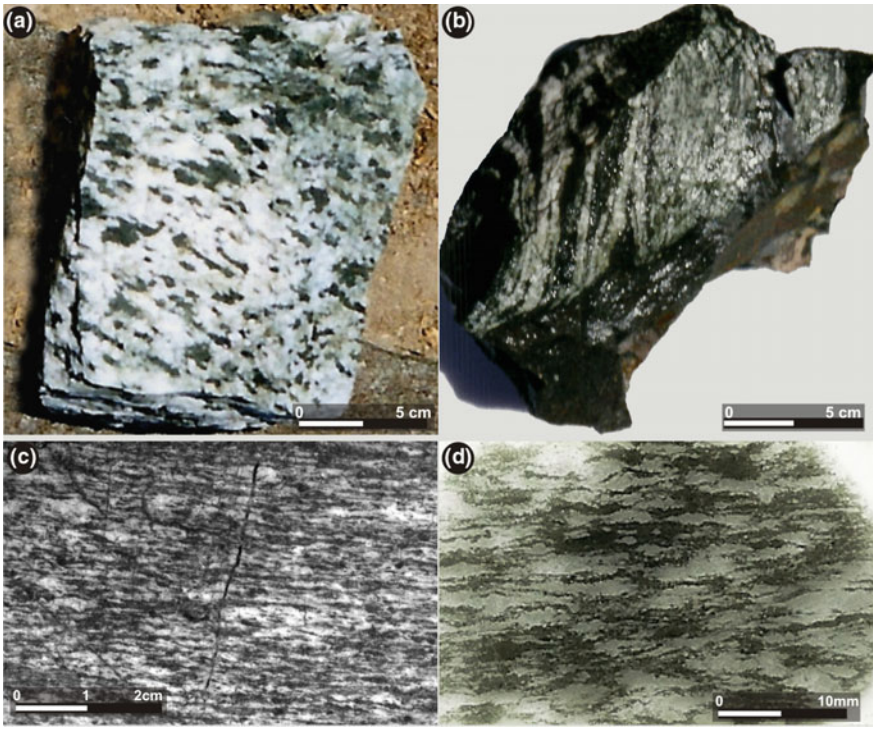

Fig. 7 **a**, **b** Hand samples of ductile-deformed gabbros; **c**, **d** detail of petrographic sections showing mylonitic texture in gabbros, from El Nihuil mafic unit

minerals. The deformed samples show recrystallized amphibole parallel to the foliation. The plagioclase is strongly altered to sericite and epidote. The tonalites are composed of zoned plagioclase (An_{38}), biotite, and quartz. The biotite is mainly

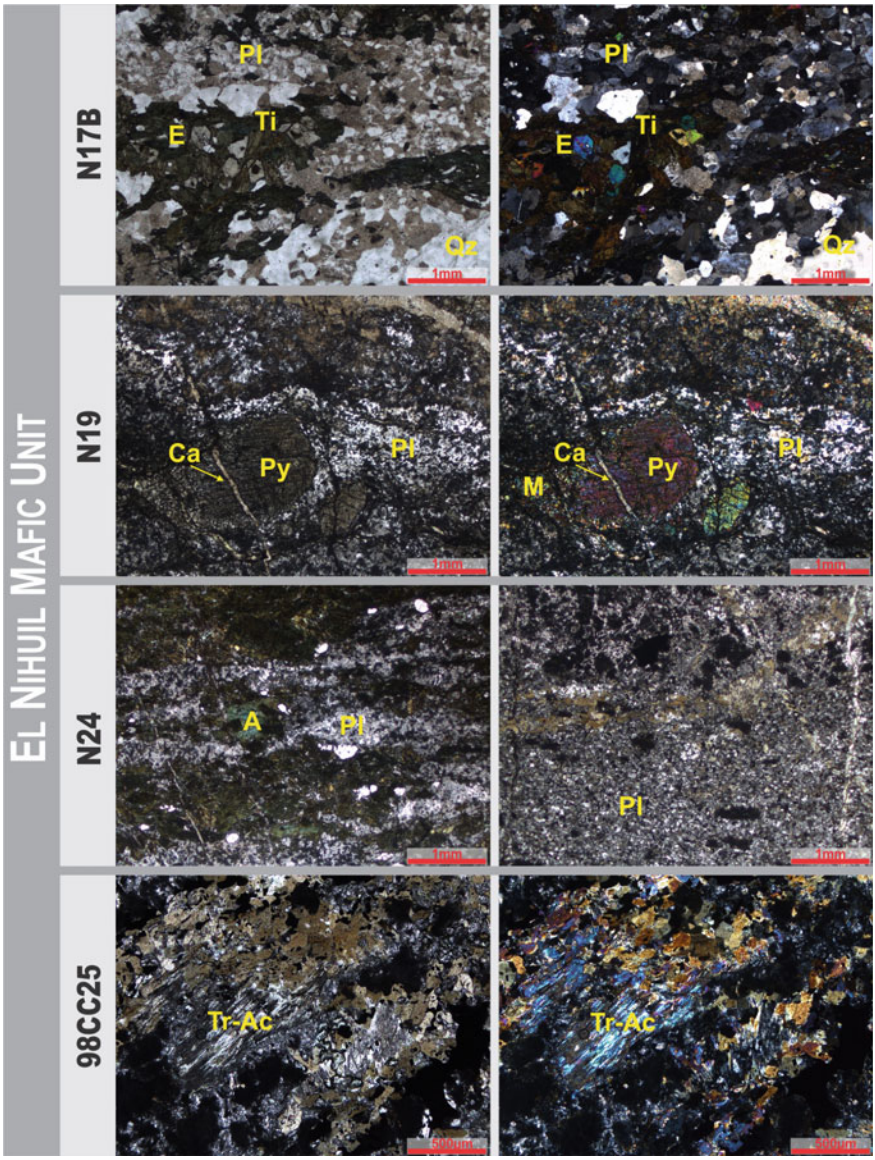
El Nihuil Mafic Unit
N17B
N19
N24
98CC25
Pl
Ti
E
Qz
Ca
Py
M
A
Tr-Ac
1mm
500µm

◂**Fig. 8** Photomicrographs (Leica DM 2500P microscope) of samples from the El Nihuil mafic unit ('Loma del Petiso shear zone' and Lomas Orientales). **N17B**: This sample shows well-oriented metamorphic fabric with 8-mm-long hornblende (*A*), with mylonite texture; quartz (*Qz*) and plagioclase (*Pl*) are also present with scarce K-feldspar, showing polygonal mosaic and lensoid texture. The porphyroclasts/porphyroblasts with quartz inclusions lensoidal granoblastic texture within a matrix of plagioclase and quartz. Accessory minerals are sphene (*Ti*) and epidote (*E*). Rock derived from mafic protolith like tonalite, quartz diorite, or quartz amphibolite. (2.5X). **N19**: Sample with pyroxene (*Py*) and plagioclase (*Pl*) as porphyroclasts, partially brecciated, and showing veins of secondary calcite (*Ca*) and with recrystallization of plagioclase. Silicification is also present. Porphyroclasts edges of pyroxene with high-temperature recrystallization forming 'mantle' (2.5X). **N24**: mafic foliated rock with hornblende (*A*), plagioclase (*Pl*) and tremolite—actinolite showing mylonitization in hydrous conditions (2.5X). **98CC25**: Rock sample with granoblastic texture, altered, and brecciated. The amphibole (*A*) was transformed in tremolite–actinolite (*Tr–Ac*). Secondary minerals are apatite and opaques. Other recognized minerals are calcite, quartz, and epidote. Equigranular texture, mylonitizated. Amphibole in mosaics and mafic phenoclasts are replaced by fibrous minerals (2.5X)

altered to chlorite and medium-grained epidote, probably related to a subsolidus crystallization event. Accessory minerals are apatite, sphene, and allanite.

We also include in this chapter, the strongly ductile-deformed gabbros and foliated granodiorite–tonalite orthogneissic samples (Fig. 6a, b) from outcrops preserved at "Loma del Petiso shear zone" and Lomas Orientales within the **El Nihuil Mafic Unit** *ca*. 45–50 km to the NW of the Ponón Trehué region (Cingolani et al. 2000). The petrological characteristics of gneissic rocks are comparable to the tonalites described at Leones River. They have a metamorphic foliation N83°W/54° SW quite similar in all gneissic outcrops suggesting that they correspond to Cerro La Ventana Formation basement relicts (preserved like enclaves or roof pendants) here intruded by Lower Paleozoic dolerites within the El Nihuil mafic unit (Fig. 3; Cingolani et al., this volume).

The basement relicts that crops out at the El Nihuil mafic unit mentioned before are composed of gabbros and tonalites–granodiorites showing mylonitic and cataclastic textures (Figs. 7a–c, 8 and 9).

The relationships with the Lower Paleozoic Ponón Trehué Fm (Fig. 2) and El Nihuil Dolerites (Fig. 3) suggest that the deformation and metamorphism affecting the Cerro La Ventana Formation should have occurred long before its exhumation during Early Ordovician and probably during the late stages of the Mesoproterozoic Grenville orogeny. During the Cenozoic, the final compressive tectonism juxtaposed through east-vergence thrusting basement rocks with both Ordovician and Upper Paleozoic units, as pointed out by Nuñez (1979; Fig. 4a).

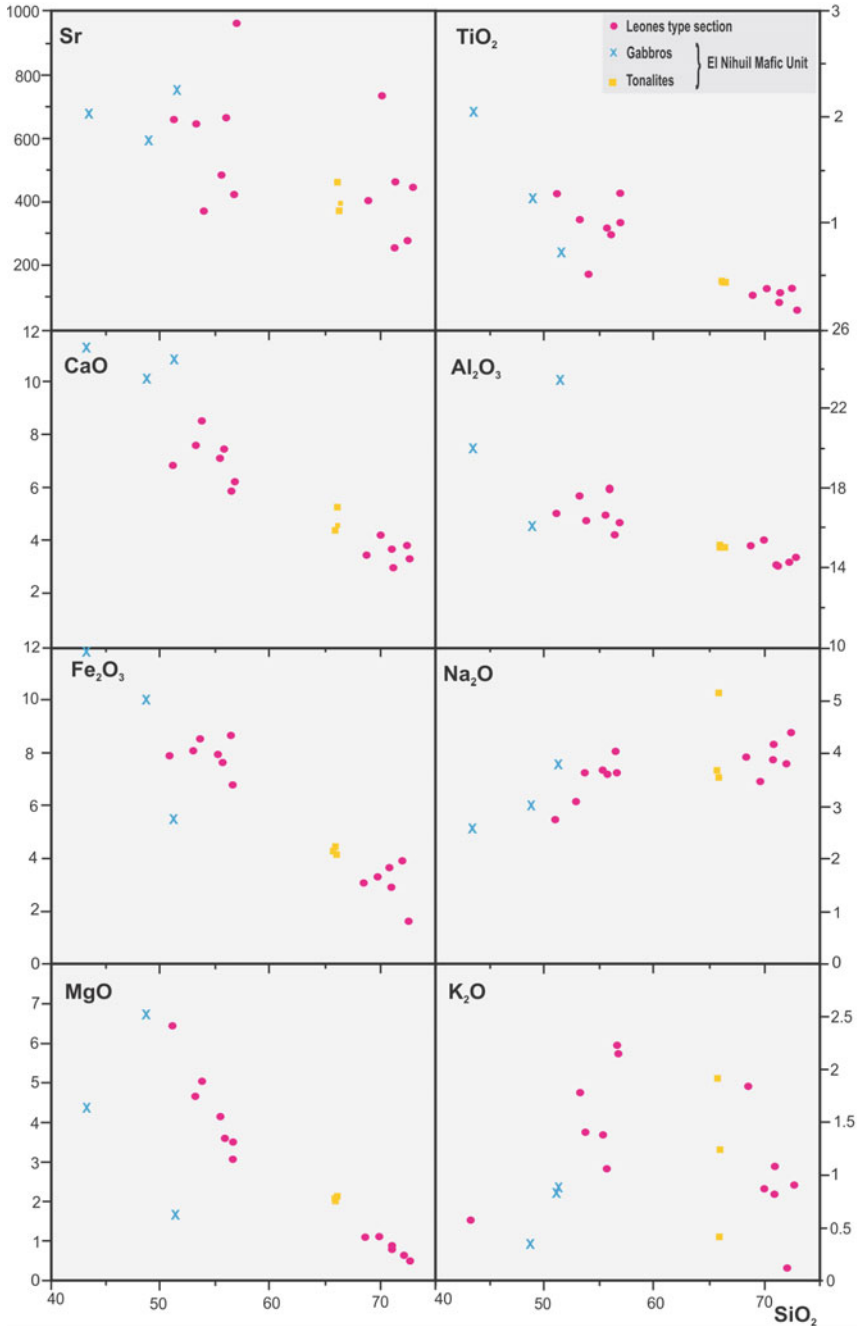

Fig. 9 Harker diagrams for the studied samples for the elements K, Na, Ti, Ca, Fe, Al, Sr, and Mg. A compositional gap can be seen between tonalites and gabbros

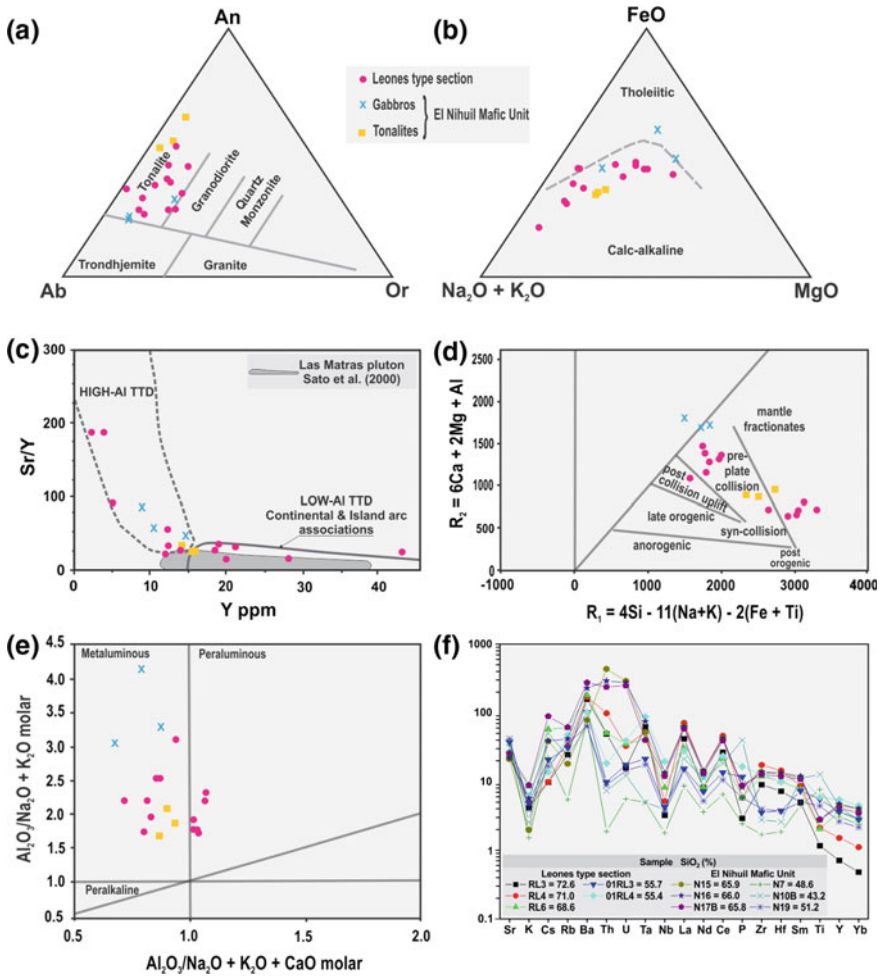

Fig. 10 **a** Classification of rocks after Barker (1979), based on normative An, Ab, Or; **b** AFM diagram showing that samples plot mainly in the calc-alkaline field after Batchelor and Bowden (1985); **c** Sr/Y versus Y diagram after Drummond and Defant (1990) showing that a half of total samples are similar to those from the Las Matras block, interpreted as low-Al TTD (Sato et al. 2000). However, samples from our work show dispersion with high Sr/Y ratios typical of high-Al TTD; **d** in the R1 versus R2 tectonic discrimination diagram the samples plot mainly in the pre-plate collision to syn-collision fields; **e** relation of A/CNK (molar) and $Al_2O_3/(Na_2O + K_2O)$ molar, showing the metaluminous/peraluminous signature of studied rocks; **f** expanded diagram of the trace elements normalized to the primitive mantle (Taylor and McLennan 1985)

6 Lithogeochemistry

6.1 Major Elements

The results of whole-rock samples from the Cerro La Ventana Formation were split into the two groups of outcrops to better describe them (Tables 2 and 3):

1. **El Nihuil Mafic Unit**, (a) tonalites (N15, N16, N17B) with SiO_2 around 66%, Al_2O_3 of 15% and Fe_2O_3 between 4.1 and 4.4%; the concentrations of all major elements are quite similar for the three samples, but a wider spread is found for K_2O and Na_2O; (b) gabbros (N7, N10B, N19) have a SiO_2 concentration varying from 43.2 to 51.1%, Al_2O_3 is in between 16 and 23.4%, Fe_2O_3 ranges from 5.4 to 11.7%, and MgO is in between 1.6 and 6.7%.
2. **Leones type section**, (a) gabbros and tonalites (CV17 to CV20, 01 RL2, 01RL4) with SiO_2 concentrations between 52.8 and 56.6%, Al_2O_3 ranges from 15.7 to 17.9%, Fe_2O_3 contents vary from 6.7 to 8.5%, while MgO is in between 3.1 and 5.1%; (b) the last group here described corresponds to the more acidic component (granodiorites) of the basement and includes samples (RL3, RL4, RL6, 01RL1) showing SiO_2 concentrations above 68.5 and up to 72.6%, Al_2O_3 is in between 14 and 15.3% and Fe_2O_3 contents vary from 1.6 to 3.9%.

Harker diagrams (Fig. 9) clearly show the behavior of major elements and Sr for all studied samples from the two groups: a positive correlation can be seen for Na_2O, whereas a negative correlation is observed for TiO_2, CaO, Fe_2O_3, Al_2O_3, and MgO. Correlations between Sr and K_2O with SiO_2 can be roughly described as negative, despite the dispersion shown. These characteristics could be indicating cogenetic rocks.

In the An-Ab-Or diagram (Fig. 10a) the rock samples plot in the field of the tonalites, although a few are close to the field of granodiorites and two tonalite enclaves from El Nihuil mafic unit plot in the field of trondhjemites close to the tonalite field; in the AFM diagram samples follow a calc-alkaline trend (Fig. 10b). Differences between samples from the type section and gabbroic samples from the El Nihuil mafic unit are evident, since the latter follow a more tholeiitic signature. The bulk of samples from the Cerro La Ventana Formation plot within the field of metaluminous rocks; although a few are in the peraluminous field, their A/CNK ratios are of 1.1 maximum (Fig. 10e). In the R1 versus R2 tectonic discrimination diagram the samples plot in the field of pre-plate collision to syn-collision (Fig. 10d). In the expanded multielement diagram normalized to primitive mantle, it is shown a coherent evolution of the LIL and HFS elements for the studied samples suggesting cogenetic events. Only the presence of the Th and U positive anomaly in the El Nihuil mafic samples show a difference (Fig. 10f).

Table 4 Analytical results of rare earth elements (ppm)

Rare earth elements											
Samples	Leones type section					El Nihuil mafic unit					
	RL-3	RL-4	RL-6	01-RL-4	01-RL1	N-7	N10-B	N-19	N15	N16	N17B
La	23.00	39.30	16.70	15.30	61.5	4.76	11.70	8.00	35.3	34.30	32.1
Ce	38.3	63.4	30.9	33.7	6.23	9.3	26.5	15.2	61.5	60.70	56.4
Pr	3.83	6.74	3.47	4.29	23	1.18	3.67	1.84	6.23	6.13	5.79
Nd	13.2	22.5	13.2	18.8	3.99	5.82	18.1	8.41	23	22.90	21
Sm	1.73	2.98	2.66	4.03	0.959	1.56	3.86	1.74	3.99	4.13	3.77
Eu	0.771	0.889	0.751	1.430	3.57	1.44	2.09	1.13	0.959	1.01	0.914
Gd	1.12	2.02	2.37	3.75	0.49	2.03	3.90	1.75	3.57	3.53	3.2
Tb	0.13	0.23	0.41	0.63	2.75	0.31	0.54	0.27	0.49	0.50	0.43
Dy	0.53	1.03	2.26	3.48	0.52	2.05	2.92	1.51	2.75	2.71	2.45
Ho	0.09	0.18	0.42	0.67	1.47	0.41	0.56	0.30	0.52	0.55	0.48
Er	0.22	0.48	1.20	1.89	0.23	1.05	1.40	0.84	1.47	1.45	1.36
Tm	0.027	0.066	0.180	0.277	1.45	0.142	0.179	0.119	0.23	0.23	0.21
Yb	0.18	0.41	1.07	1.67	0.253	0.88	1.01	0.80	1.45	1.51	1.28
Lu	0.026	0.060	0.140	0.233		0.141	0.153	0.117	0.253	0.24	0.208
Sum	83.15	140.29	75.73	90.15	106.41	31.07	76.58	42.03	141.71	139.88	129.59
Sm_n	7.49	12.90	11.52	17.45		6.75	16.71	7.53	17.27	17.88	16.32
Eu_n	8.86	10.22	8.63	16.44		16.55	24.02	12.99	11.02	11.61	10.51
Gd_n	3.66	6.60	7.75	12.25		6.63	12.75	5.72	11.67	11.54	10.46
$s*g_n$	27.41	85.16	89.19	213.80		44.80	212.97	43.08	201.52	206.25	170.67
Eu/Eu*	1.69	1.11	0.91	1.12		2.47	1.65	1.98	0.78	0.81	0.80

$Eu_N/Eu^* = Eu_N/(0.67Sm_N + 0.33Tb_N)$

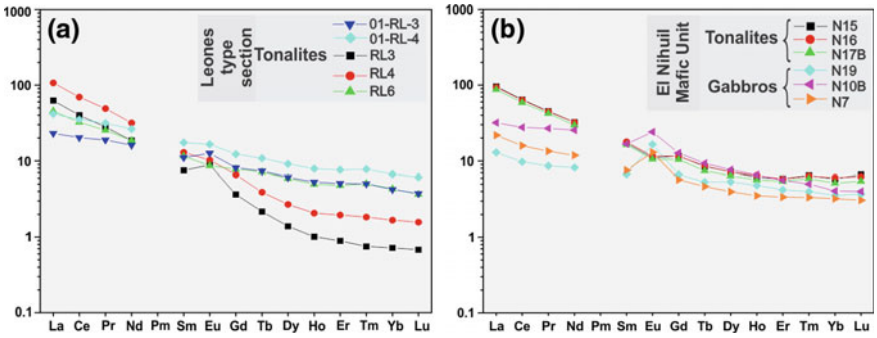

Fig. 11 Chondrite-normalized REE diagrams for, **a** Leones type section; **b** El Nihuil mafic unit. Normalization values from Taylor and McLennan (1985)

6.2 Trace and Rare Earth Elements

Sr/Y versus Y is a useful diagram (Fig. 10c) to discriminate between high and low-Al tonalite–trondhjemite—dacite (TTD) complexes. Main groups of samples plot accordingly to rocks from the Las Matras block (Sato et al. 2000), as low-Al TTD; however, some samples show high Sr/Y ratios which are typical of high-Al TTD in agreement with the diagram of Drummond and Defant (1990).

Samples from the type section of the Cerro La Ventana Formation as well as those from mafic and felsic deformed relicts included in the El Nihuil mafic unit are characterized by high values of Mg# (Mg/Mg + Fe molar ×100; gabbros: 65–67, tonalites 55–70), with respect to rocks with similar silica contents, including those from the Las Matras TTG (Sato et al. 2000, 2004). Furthermore, the Mg# is higher to that produced by slab melts at 1.4 GPa with a residue of gt + cpx ± amph and is superposed with the hybridized slab melts and high magnesia adakites fields, according to Rapp et al. (1999). In order to describe the grade of magnesium enrichment with respect to other differentiated magma, the Mg#/K molar versus silica was plotted. Both the low and high silica rocks studied show similar Mg enrichment respect to K, signature which allows linking both groups of rocks to a same igneous evolution. The Mg#/K ratio is higher for the Cerro La Ventana Formation compared with Las Matras TTG series, suggesting a lower grade of differentiation for the first unit. In the R1 versus R2 diagram the tonalites and diorites from Leones type section plot in two separate groups. The rocks from the crustal enclaves included in El Nihuil mafic unit behave similarly to the tonalites (Fig. 10d). Samples from Leones creek have La/Yb_N ratios in between 5.5 and 86.3 and Eu_N/Eu^* ranges from 0.9 to 1.7; their chondrite-normalized REE diagram (Table 4; Fig. 11a) shows rather positive Eu anomalies. Samples from the El Nihuil

Table 5 Rb–Sr isotopic data from samples of the Cerro La Ventana type section and El Nihuil mafic unit

	Lab. N°	Field N°	Rb (ppm)	Sr (ppm)	$^{87}Rb/^{86}Sr$	Error	$^{87}Sr/^{86}Sr$	Error
Leones type section	CIG 1003	RL1	16.1	263.7	0.1767	0.0049	0.70598	0.00007
	CIG 1004	RL2	14	288.2	0.1406	0.0039	0.70524	0.00012
	CIG 1005	RL3	13.3	482.6	0.0798	0.0022	0.70409	0.00008
	CIG 1006	RL4	19.3	508.1	0.1099	0.0031	0.70495	0.00009
	CIG 1007	RL5	36.4	449	0.2347	0.0066	0.70667	0.00009
	CIG 1008	RL6	34.3	436.3	0.2276	0.0064	0.70675	0.00009
	CIG 1009	PT1	25.8	265.1	0.2817	0.0079	0.70734	0.00009
	CIG 1015	RL1 D	16.1	263.7	0.1767	0.0049	0.70598	0.00011
	CIG 1016	RL3 D	13.3	482.6	0.0798	0.0022	0.70426	0.00012
El Nihuil Mafic Unit	CIG 1104	N19	23	787.5	0.0845	0.0017	0.704338	0.000028
	CIG 1105	99S22	28.6	492.5	0.1681	0.0034	0.70633	0.000019
	CIG 1197	99S18	7.8	348.6	0.0648	0.0013	0.703779	0.000035
	CIG 1201	N 7	4.3	603.9	0.0206	0.0004	0.703228	0.000063
	CIG 1203	N 19′	21.2	781.1	0.0786	0.0016	0.704282	0.000049
	CIG 1204	99S22′	25.8	480.7	0.1554	0.0031	0.706366	0.000035

mafic unit shows patterns depleted in HREE (Fig. 11b), with La/Yb_N ratios in between 15.3 and 16.9. Therefore, they are dissimilar to diorites from the same unit, which develop REE patterns parallel to N-MORB and have La/Yb_N ratios lower than 1.4. Gabbros display patterns with positive Eu anomalies typical of plagioclase-rich igneous rocks.

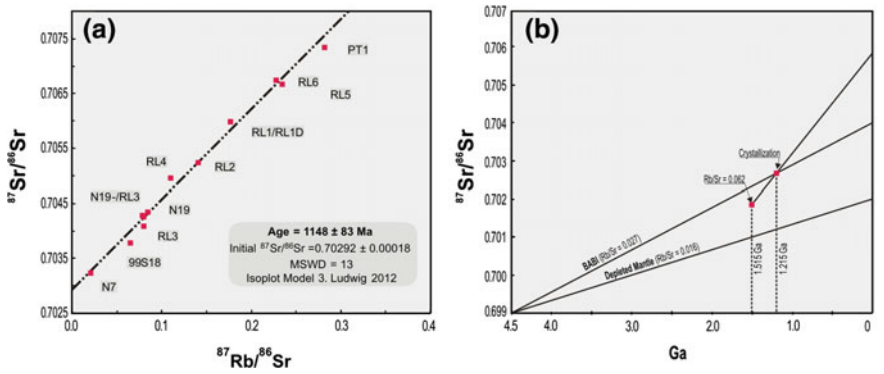

Fig. 12 **a** Rb–Sr isochronic diagram using Isoplot Model 3 by Ludwig (2012) on samples from Leones type section (RL 2, RL 3, RL 5, RL 6, and PT1) and from El Nihuil mafic unit (N7, N19, 99S18). **b** Linear $^{87}Sr/^{86}Sr$ evolution of BABI and of a depleted mantle through time (Faure 1986). The initial $^{87}Sr/^{86}Sr$ found for Cerro La Ventana Fm including samples from El Nihuil mafic unit (0.7029) suggest a derivation from mantle represented by BABI (Rb/Sr = 0.027) considering a 1.2 Ga crystallization age. Another explanation could be refusion of a magma (with Rb/Sr = 0.047) extracted from depleted mantle (Rb/Sr = 0.016) at *ca*. 1.5 Ga

7 Isotopic Data

Rb–Sr: The Rb–Sr systematic was applied by Cingolani and Varela (1999) on 7 whole-rock samples (RL1, RL2, RL3, RL4, RL5, RL6, and PT1), from the granodioritic–tonalitic facies outcropping at the type section of the Cerro La Ventana Formation along Leones and Ponón-Trehué creeks. The Rb concentrations are rather low and vary between 13.3 and 36.4 ppm, while Sr concentrations are high and range from 263.7 to 508.1 ppm; therefore, the $^{87}Rb/^{86}Sr$ ratios are between 0.0798 and 0.2817. According to the model from Williamson (1968), the isochrone age is 1063 ± 106 Ma, and the initial ratio $^{87}Sr/^{86}Sr$ is of 0.7032 ± 0.0003 with MSWD of 1.06. Data recalculated using the Isoplot Model 3 (Ludwig 2012) show an alignment within a low range of $^{87}Rb/^{86}Sr$ (<0.3); the age obtained is 1109 ± 130 Ma (1sigma), initial ratio $^{87}Sr/^{86}Sr$: 0.70304 ± 0.00032, and MSWD of 7.4 (Cingolani and Varela 1999).

Four samples from the El Nihuil mafic unit (N19, 99S22, 99S18 and N7), considered as part of the basement, were recently added (Table 5; Fig. 12a). They show Rb concentrations in between 4.3 and 28.6 ppm, while the Sr concentrations range from 348.6 to 787.5 ppm; the $^{87}Rb/^{86}Sr$ ratios are between 0.0206 and 0.1681. Comparing to data from the type section of the Cerro La Ventana Formation, the El Nihuil mafic unit has lower Rb and higher Sr contents. Using all samples from both regions altogether (excluding 99S22 since it is out of the linear isochrone) following Isoplot Model 3 (Ludwig 2012), an isochron with 1148 ± 83 Ma (1sigma), initial $^{87}Sr/^{86}Sr$ ratio of 0.70292 ± 0.00018, and MSWD = 13 is recorded (Fig. 11a). The low initial $^{87}Sr/^{86}Sr$ ratio is indicative of a

Table 6 Sm-Nd isotopic data for samples taken at Leones type section and El Nihuil Mafic Unit (N15)

Sample	Sm (ppm)	Nd (ppm)	$^{147}Sm/^{144}Nd$	Error	$^{143}Nd/^{144}Nd$	Error (2σ)	$\varepsilon_{Nd(0)}$	$f_{Sm/Nd}$	ε_{Nd} (t = 1.2 Ga)	T^a_{DM} (Ma)	ε_{NdTDM}
CV17	2.092	14.104	0.0897	0.0005	0.511996	0.000010	−12.52	−0.54	3.86	1286.8	5.05
CV18	3.146	14.452	0.1316	0.0008	0.512338	0.000012	−5.86	−0.33	4.10	1308.4	5.00
CV19	3.197	14.240	0.1358	0.0008	0.512381	0.000010	−5.00	−0.31	4.32	1291.9	5.04
CV20	3.497	14.221	0.1487	0.0009	0.512503	0.000006	−2.64	−0.24	4.71	1264.1	5.10
N15	3.29	18.88	0.1052	nd	0.511872	nd	−14.94	−0.46	−0.94	1640.0	4.2
RL2	1.46	8.91	0.099344	nd	0.512031	0.000019	−11.84	−0.50	3.1	1345.3	4.91
RL3	1.63	12.75	0.078509	nd	0.511939	0.000012	−13.63	−0.61	4.64	1234.8	5.17
RL4	3.01	22.85	0.079511	nd	0.511863	0.000016	−15.12	−0.60	2.8	1341.9	4.92
RL5	1.85	8.20	0.136597	nd	0.512370	0.000021	−5.22	−0.31	4.0	1325.1	4.96
PT1	2.01	16.17	0.075173	nd	0.511902	0.000027	−14.36	−0.62	4.25	1256.3	5.12

T^a_{DM}: based on De Paolo (1981) ($^{146}Nd/^{144}Nd = 0.7219$); $Epsilon_{Nd(0)} = \{[(^{143}Nd/^{144}Nd)_{sample}/0.512638] - 1\} \times 10^4$, where $^{143}Nd/^{144}Nd_{CHUR} = 0.512638$. $f_{Sm/Nd} = \{[(^{147}Sm/^{144}Nd)_{sample}/0.1967)] - 1\}$, where $^{147}Sm/^{144}Nd_{CHUR} = 0.1967$ (Hamilton et al. 1983). *nd* no data

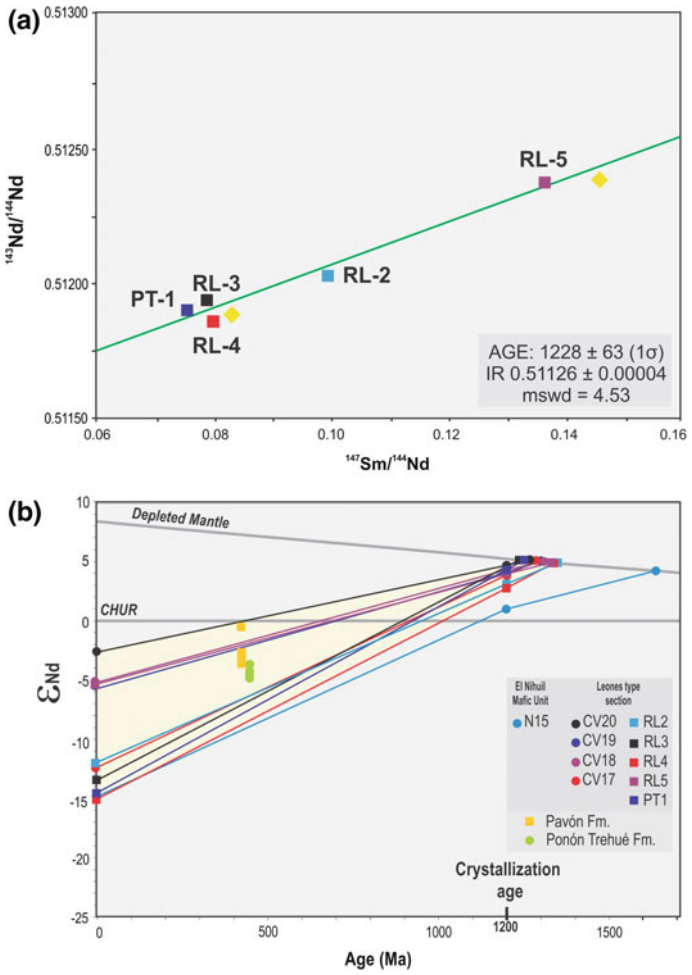

Fig. 13 **a** Sm-Nd isochron diagram from Cerro La Ventana Formation type section samples. **b** ε_{Nd} data for samples from Leones type section and El Nihuil Mafic Unit. Data of Ordovician sequences (Pavón and Ponón Trehué Fms) are also shown (Abre et al. 2011; Abre et al., this volume)

slight evolved Mesoproterozoic source for the tonalitic rocks sampled at Leones and Ponón Trehué creeks as well as for samples from the El Nihuil mafic unit.

If we consider a linear strontium isotopic evolution of BABI through time with $^{87}Sr/^{86}Sr$ from 0.699 to 0.704 (Rb/Sr = 0.027; Faure 1986) during the 4.5 Ga, the $^{87}Sr/^{86}Sr$ value for *ca*.1.2 Ga (crystallization age) is close to the value of 0.70292 ± 0.00018 obtained from the Rb–Sr isochronic diagram (Fig. 12b). This could suggest a direct mantle derivation for the magma at this time. The low $^{87}Sr/^{86}Sr$ ratios as well as the Potassium contents and high Mg# permit to interpret that the studied samples are juvenile rocks (less evolved), similar to the modern

Table 7 Pb–Pb analytical isotopic data of samples from the Cerro La Ventana Fm

Sample	$^{206}Pb/^{204}Pb$	Error[a]	$^{207}Pb/^{204}Pb$	Error[a]	$^{208}Pb/^{204}Pb$	Error[a]
CV17	16.965	0.014	15.398	0.017	37.239	0.020
CV18	17.800	0.013	15.473	0.014	36.685	0.015
CV19	17.580	0.009	15.464	0.011	36.749	0.012
CV20	20.319	0.010	15.684	0.010	38.385	0.010

Isotopic ratios corrected for 0.095%/u.m.a mass fractionation; error[a]: standard relative error (60 measurements in average); total blank during measurements = 119 pg; average isotopic ratios of standard NBS-981 including a deviation of 1sigma (01–08/2010): $^{206}Pb/^{204}Pb = 16.898 \pm 0.003$; $^{207}Pb/^{204}Pb = 15.440 \pm 0.003$; $^{208}Pb/^{204}Pb = 36.542 \pm 0.010$

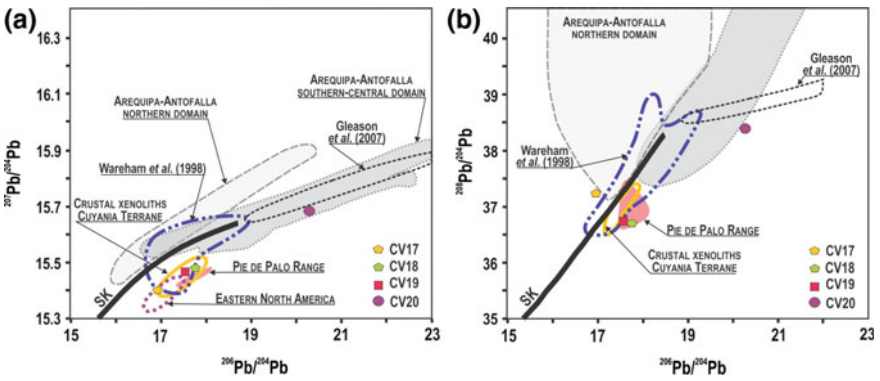

Fig. 14 **a**, **b** Pb isotopes of the Cerro La Ventana Fm samples and other basement regions of South America (Ramos 2004). Note that the samples CV17, CV18, and CV19 have distinctive nonradiogenic signature near the field of Pie de Palo complex rocks and crustal xenoliths of Cuyania Terrane; SK = lead isotope curves after Stacey and Kramers (1975)

adakites or Precambrian TTD series. In this sense, are equivalents to the "Grenvillian-age" Las Matras tonalite–trondhjemite pluton (Sato et al. 2000, 2004; Varela et al. 2011).

Sm–Nd: Samples selected for whole-rock Sm–Nd isotopic analyses performed at the Laboratorio de Geología Isotópica, Porto Alegre-Brazil, comprise basement rocks from the Leones (type section of Cerro La Ventana Formation: CV17 to CV20, RL2 to RL5 and PT1) as well as one from the El Nihuil mafic unit (sample N15; Table 6). This isotopic work emphasized the crustal residence (T_{DM}) age determinations and allows us to recognition crustal segments to understand the history of tectonic accretion.

An acceptable isochron was obtained using five Sm–Nd analyses and two duplicates (Fig. 13a), indicating an age of 1228 ± 63 Ma (1 sigma), and MSWD 4.53 and initial $^{143}Nd/^{144}Nd$ 0.51126 ± 0.00004. The model ages (T_{DM}) calculated according to DePaolo (1981) for ten samples are in the range 1.23–1.64 Ga. The $\varepsilon Nd_{(1200)}$ for these samples (Fig. 13b) is in between −0.94 and +4.7 indicating a 'depleted' source, less evolved than CHUR for the time of crystallization, which is

Table 8 U–Pb analytical data and typology of zircons studied by isotope dilution and TIMS methodology at University of São Paulo, Brazil

SPU	Magnetic fraction	Mineral typology	207/235[a]	Error (%)	206/238[a]	Error (%)	Coef.	238/206	Error (%)	207/206	Error (%)	206/204[b]	Pb (ppm)	U (ppm)	Weight (m)	206/238 Age (Ma)	207/235 Age (Ma)	207/206 Age (Ma)
02-RL-103 RIO SECO DE LOS LEONES																		
2164	D	P(2-4/1), Fr, T, Ambar, cl, CI, l, F	2.28546	0.49	0.205677	0.484	0.98916	4.86199235	0.484	0.080591	0.0719	5929.2	79.3	385.2	0.037	1206	1208	1212
2165	E	P (2-1.5/1), T, Ot, Pink, CI, I, F	2.26035	0.481	0.203087	0.477	0.99332	4.92399809	0.477	0.080722	0.0554	4919.5	76.7	348.1	0.028	1192	1200	1215
2161	A	Py(1.5/1), T, Pink, CI	2.29936	0.487	0.206338	0.487	0.99222	4.84641704	0.484	0.080821	0.0607	3124.1	36.5	176.4	0.037	1209	1212	1217

Typology—Zircon

Shape		Color/Transparency		Internal features	
P(x/y)	Prismatic crystals	T	Transparent crystals	CI	Crystal with no or few inclusions or fractures
Py	Prismatic crystals with well-developed pyramidal facets	Ot	Opaque or translucent crystal	I	Crystal with frequent inclusions
Fr	Crystals fragments			F	Crystal with frequent fractures

SPU: laboratory number

Magnetic fractions: numbers in parentheses indicated the tilt used on Frantz separator at 1.5 A current

[a]Radiogenic Pb corrected for blank and initial Pb; U corrected for blank;

[b]Not corrected for blank or nonradiogenic Pb

Total U and Pb concentrations corrected for analytical blank

Ages: given in Ma using Ludwig Isoplot/Ex program (1998), decay constants recommended by Steiger and Jäger (1977)

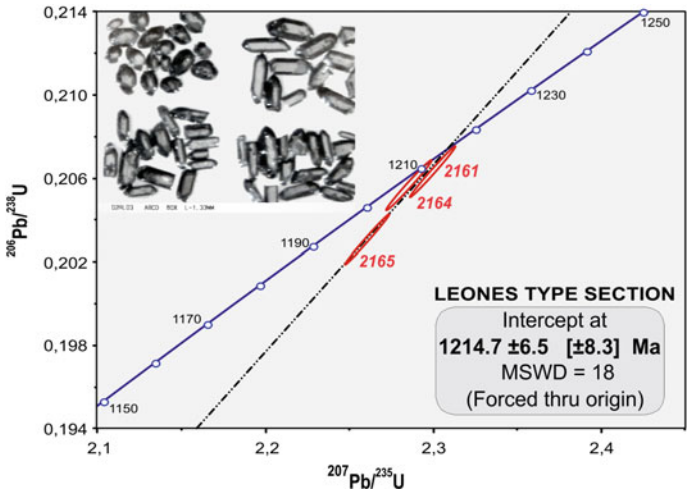

Fig. 15 Concordia plot of zircons from Leones sample analyzed by isotope dilution and TIMS methodology at University of São Paulo, Brazil. In the inset the microscope image of zircon fractions

rather similar to the immature source for the orthogneisses found in Western Pampean Ranges (Sato et al. 2000; Ramos 2004). Dating obtained from both, Sm–Nd and Rb–Sr methods are roughly coincident within errors, indicating that an average age of 1200 Ma can be reasonably proposed as crystallization age for the Cerro La Ventana Formation with contribution of juvenile material.

Pb–Pb: Pb analyses were performed on four whole-rock samples from the Cerro La Ventana Formation (CV17 to CV20); $^{206}Pb/^{204}Pb$ range from 16.965 to 20.319, $^{208}Pb/^{204}Pb$ range from 36.685 to 38.385, whereas the radiogenic lead ($^{207}Pb/^{204}Pb$) is in between 15.398 and 15.684 (Table 7). Samples from the Cerro La Ventana Formation plot in a $^{207}Pb/^{204}Pb$ diagram (Fig. 14a) below the Stacey and Kramers (1975) second-stage Pb evolution curve for average crust, similar to rocks from the basement of Cuyania Terrane (Pie de Palo Range and crustal xenoliths). In a $^{208}Pb/^{204}Pb$ diagram (Fig. 14b) most of the samples also plot below the second-stage Pb evolution curve for average crust as basement rocks from the Cuyania Terrane, except for sample CV17 which is above such a curve. Although sample CV20 (garnet it was described on thin section) remains below SK curve, it shows the higher Pb ratios, particularly regarding $^{206}Pb/^{204}Pb$, and being therefore dissimilar to crustal xenoliths and Pie de Palo rocks from the basement of the Cuyania Terrane.

U–Pb: Two methods were applied: the isotope dilution (ID) with thermal ionization mass spectrometry (TIMS) and in situ LA-ICP-MS as follow:

(a) **ID-TIMS**: A sample of the tonalitic facies located at Leones River type section (01RL03) with 55.78% of SiO_2 was chosen for zircon U–Pb TIMS dating. The analyses were carried out at the Centro de Pesquisas Geocronológicas, São

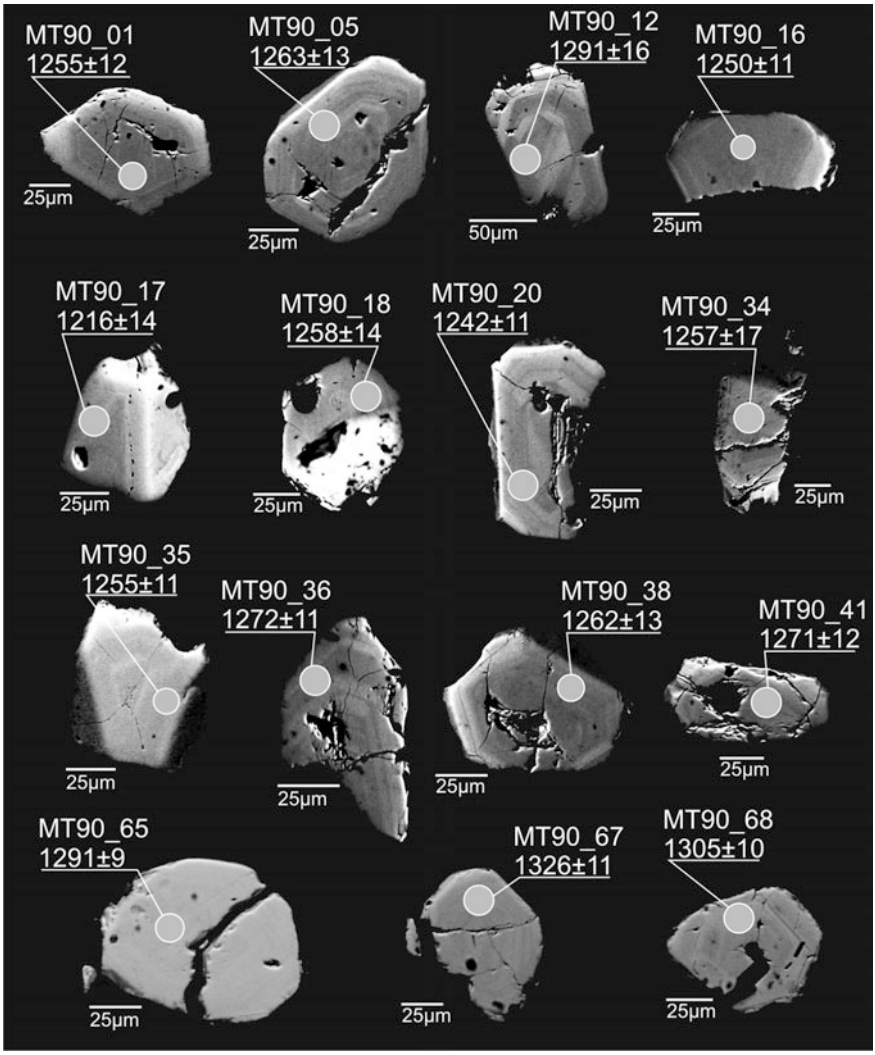

Fig. 16 Backscattering images of selected zircon crystals with spot locations by LA-ICP-MS analyses at LGI-UFRGS, Porto Alegre, Brazil laboratory. Ages in Ma

Paulo, Brazil. Four zircon fractions (Table 8; Fig. 15) were analyzed, with prismatic, euhedric and well-developed crystal faces. All were transparent crystals without inclusions or fractures. The obtained age of 1214.7 ± 6.5 Ma was based on main concordant 2161 and 2164 fractions and 2165 fraction with little Pb lost. The 2162 fractions with probable Pb crustal heritage were not considered in the age determination. The Mesoproterozoic obtained value is

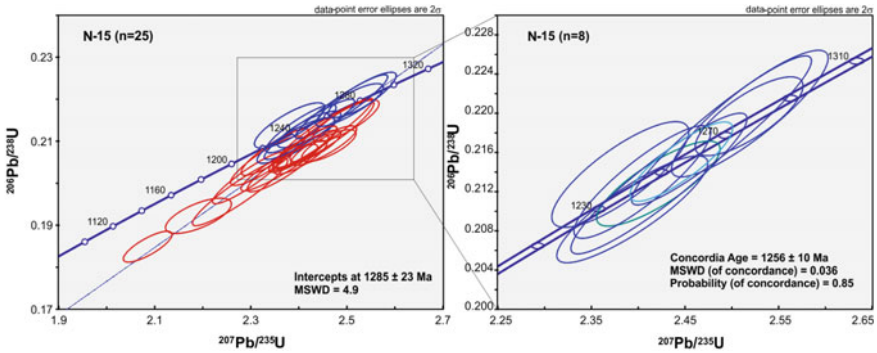

Fig. 17 Concordia plot of zircons from the sample N15 (n = 25) from El Nihuil mafic unit; on the right detail of eight concordant results

interpreted as the zircon crystallization age during the emplacement of the tonalitic magmatic rock.

(b) **LA-ICP-MS**: At the region of Lomas Orientales as part of the El Nihuil mafic unit (Cingolani et al. 2012b) crop out a meter-scale relics of tonalite–orthogneissic rocks with intermediate composition (SiO_2 around 66%) bearing a foliation with N83°W/54°SW (Fig. 5). The in situ U–Pb (LA-ICP-MS) zircon data on the sample N15 was obtained at the Laboratorio de Geología Isotópica, Universidade Federal do Río Grande do Sul, Porto Alegre, Brazil. The results yielded a $^{207}Pb/^{208}Pb$ weighted mean age of 1285 ± 23 Ma based on 25 spots (Fig. 16; Table 9). The zircon grains vary from colorless to brown, and are prismatic and subhedral with few inclusions. Some grains show rounded terminations. Backscattering images reveal that most grains display oscillatory zoning (Fig. 16). Some grains exhibit metamictization in their central part. Cracks are relatively common. The data point out a Mesoproterozoic crystallization age when all 25 results are plotted despite some scatter illustrated by the relatively high MSWD (Fig. 17a). Nevertheless, seven concordant results yielded a 1256 ± 10 Ma Concordia age (Fig. 17b) that can be considered the crystallization time.

The sample N15-N17B (tonalitic orthogneiss) taken at the same locality of Lomas Orientales along the El Nihuil mafic unit was analyzed by the in situ U–Pb (LA-ICP-MS) zircon data at the Centro de Pesquisas Geocronológicas, São Paulo, Brazil (Fig. 18). The obtained age plotted in a Tera-Wasserburg diagram is 1222.8 ± 6.9 Ma (n = 26) and record MSWD (concord.) = 0.8 (Fig. 19; Table 10) with 2 sigma errors. With these U–Pb isotopic data we confirm Rb–Sr and Sm–Nd age showing the Mesoproterozoic (boundary of Ectasian- Stenian Periods, after the IUGS International Chronostratigraphic Chart 2015) basement rocks of the San Rafael Block. The obtained age *ca.* 1.2 Ga is interpreted as a Grenvillian (Mesoproterozoic) zircon crystallization age for the Cerro La Ventana Formation and it is quite similar to those belonging to the basement of other regions from the

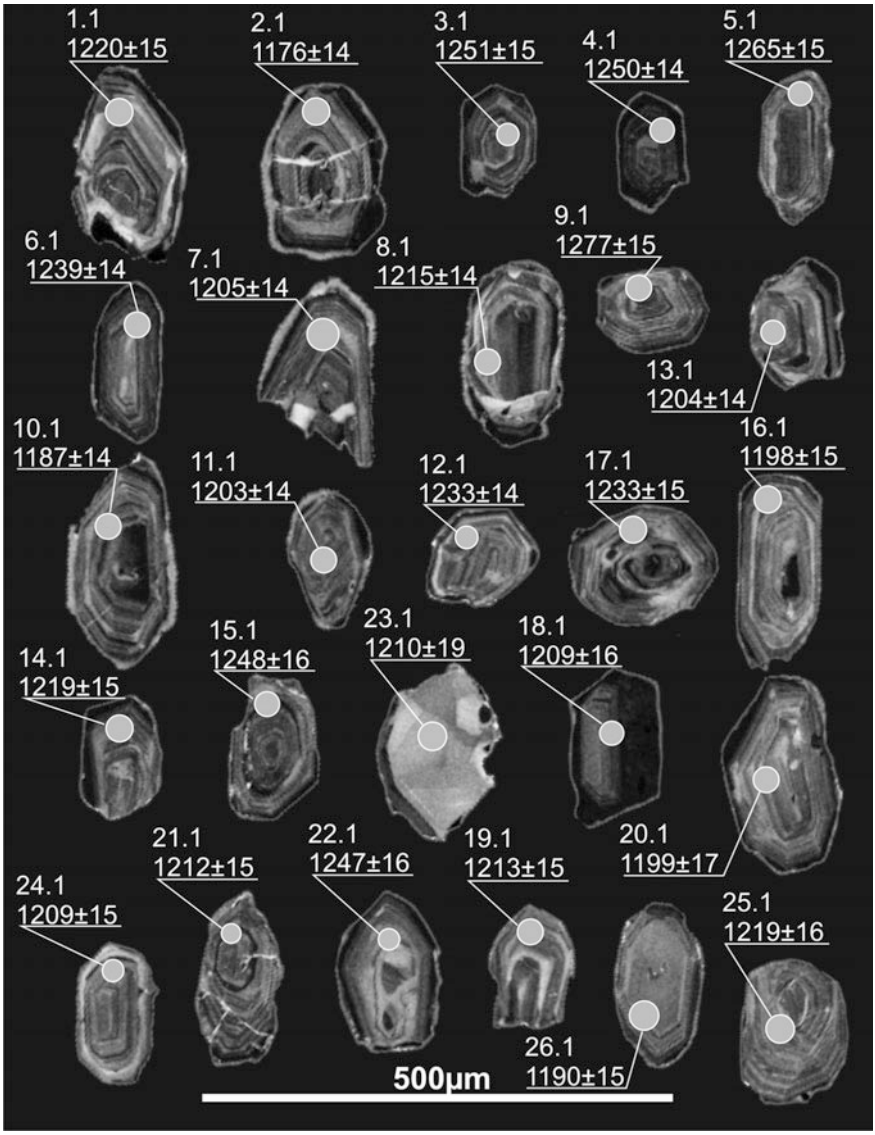

Fig. 18 Cathodoluminiscence (CL) images of selected zircon crystals with spot locations by LA-ICP-MS analyses at CPGeo-USP, São Paulo, Brazil laboratory. Ages in Ma

Cuyania allochthonous terrane (Ramos 2004; Sato et al. 2004; Morata et al. 2010; Varela et al. 2011 and references). Rapela et al. (2010) recognized in Western Pampean Ranges and Precordilleran xenoliths that the Mesoproterozoic geodynamic history evolved during 300 Ma, with a complex orogenic evolution dominated by convergent tectonics and accretion of juvenile oceanic arcs to the continent

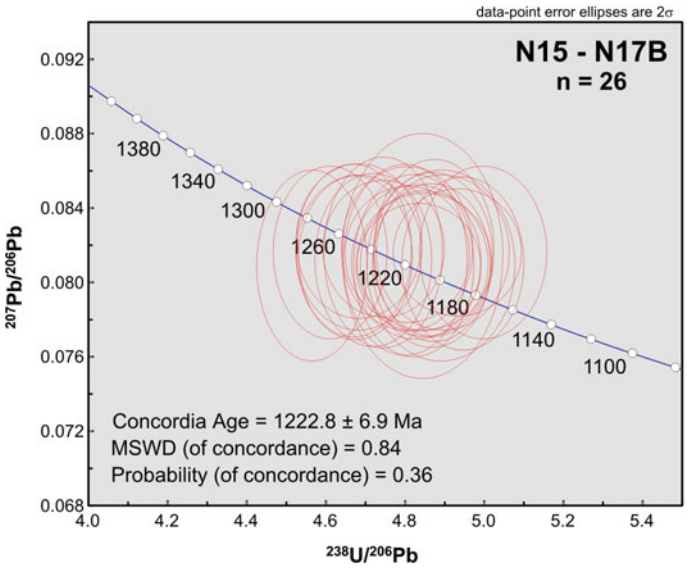

Fig. 19 Tera–Wasserburg diagram showing the plot of zircons from the sample N15-N17B from El Nihuil mafic unit

and intraplate magmatism. On the other hand Kumar et al. (2007) proposed a global thermal event at 1.1 Ga as responsible for the development of widespread global magmatic activity during this time.

8 Final Remarks

In summary, having interpreted all data presented the following statements can be drawn,

(a) The San Rafael Block crustal basement called Cerro La Ventana Formation crops out in two localities, at the Leones (type section) and within El Nihuil mafic unit, both areas showing ductile deformation.
(b) The outcrops at the type section record the primary contact between the basement and Ordovician platform sedimentary rocks, which is unique within the Cuyania terrane.
(c) The Cerro La Ventana Formation corresponds to a metamorphosed volcano-plutonic complex with hardly any sedimentary protolith that reached the high greenschist–amphibolite facies.
(d) The ductile deformation coeval with the metamorphism resulted in the folding of the complex and developed a penetrative foliation, which should have occurred long before its exhumation during Early Ordovician and probably

during the late stages of the Mesoproterozoic Grenville orogeny. This is a clear difference with Las Matras pluton from which no thermal overprint has been reported.

(e) Geochemical data indicate that the Cerro La Ventana Formation comprises cogenetic rocks with a main calc-alkaline and metaluminous character. The bulk of samples have Sr/Y ratios typical of low-Al TTD, although some can be described as high-Al TTD. The Mg#/K ratio is higher in the Cerro La Ventana Formation compared with Las Matras TTG series suggesting less differentiation for the first one. The chondrite-normalized REE diagrams for Leones samples have Eu anomalies rather positive and gabbros from El Nihuil region display patterns with positive Eu anomalies typical of plagioclase-rich igneous rocks.

(f) The Rb–Sr data defined an isochron with 1148 ± 83 Ma, initial $^{87}Sr/^{86}Sr = 0.70292 \pm 0.00018$. The low initial ratio is indicative of a slight evolved Mesoproterozoic source. An acceptable isochron was obtained using Sm–Nd methodology indicating an age of 1228 ± 63 Ma. The model ages (T_{DM}) are in the range 1.23–1.64 Ga with Epsilon $Nd_{(1200)}$ in between −0.94 and +4.7 recording a 'depleted' source, less evolved than CHUR for the time of crystallization.

(g) In Pb–Pb diagrams studied samples from the Cerro La Ventana plot similar to the rocks from the basement of Cuyania Terrane (Pie de Palo Range and crustal xenoliths) showing a distinctive nonradiogenic signature such as the Grenvillian belt of eastern Laurentia.

(h) The tonalitic facies located at the Leones River type section was chosen for zircon U–Pb TIMS dating and the obtained crystallization age is 1214.7 ± 6.5 Ma. The in situ U–Pb (LA-ICP-MS) zircon data from El Nihuil Mafic Unit (orthogneisses), analyzed in two different laboratories, plotted in a Concordia diagram record an intercept at 1256 ± 10 Ma, and the second age plotted in a Tera–Wasserburg diagram is 1222.8 ± 6.9 Ma.

(i) The isotopic data confirm the Mesoproterozoic age for the basement of the San Rafael Block; this age can also be found in basement rocks of other regions considered as part of the Laurentia derived Cuyania terrane in the proto-Andean margin of Gondwana.

Acknowledgements Field and laboratory works were financially supported by CONICET (grants PIPs 0647, 199), ANPCyT (grant PICT 07-10829) and University of La Plata (Projects 11/573, 11/704). We thank to colleagues Pablo González, Leandro Ortiz, and Diego Licitra for field work assistance and suggestions on metamorphic structural data. Luis Dalla Salda during 2001–2003 period and Alejandro Ribot, more recently, provide their expertise in discussion on petrographic description of samples. Thanks to Marcio Pimentel and Koji Kawashita for helping us in U–Pb laboratory work and data interpretation. Mario Campaña helps us with technical assistance. We are grateful to Víctor Ramos for his comments and discussions. Finally, we acknowledge to Agapito Aguilera and Domingo Solorza as field guide experts ('baqueanos') near the Leones River and El Nihuil town.

References

Abre P, Cingolani CA, Zimmermann U, Cairncross B, Chemale Jr F (2011) Provenance of Ordovician clastic sequences of the San Rafael Block (Central Argentina), with emphasis on the Ponón Trehué Formation. Gondwana Res 19(1):275–290

Abre P, Cingolani CA, Uriz NJ (this volume) Sedimentary provenance analysis of the Ordovician Ponón Trehué Formation, San Rafael Block, Mendoza-Argentina. In: Cingolani C (ed) Pre-Carboniferous evolution of the San Rafael Block, Argentina. Implications in the SW Gondwana margin. Springer, Berlin

Astini R, Ramos VA, Benedetto JL, Vaccari NE, Cañas FL (1996) La Precordillera: un terreno exótico a Gondwana. 13° Congreso Geológico Argentino y 3° Congreso de Exploración de Hidrocarburos, 5:293–324. Buenos Aires

Astini RA (2002) Los conglomerados basales del Ordovícico de Ponón Trehué (Mendoza) y su significado en la historia sedimentaria del terreno exótico de Precordillera. Revista de la Asociación Geológica Argentina 57:19–34

Barker F (1979) Trondhjemite: definition, environment, and hypotheses of origin, pp 1–12. In Barker F (ed) Trondhjemites, dacites, and related rocks. Elsevier, Amsterdam, 659 p

Batchelor AR, Bowden P (1985) Petrogenetic interpretation of granitoid rock series using multicationic parameter. Chem Geol 48(1985):43–55

Bordonaro OL, Keller M, Lehnert O (1996) El Ordovícico de Ponon-Trehue en la provincia de Mendoza (Argentina): redefiniciones estratigráficas. 12° Congreso Geológico Argentino y 2° Congreso de Exploración de Hidrocarburos 1:541–550

Bühn B, Pimentel MM, Matteini M, Dantas EL (2009) High spatial resolution analysis of Pb and U isotopes for geochronology by laser ablation multi-collector inductively coupled plasma mass spectrometry (LA-MC-IC-MS). Anais da Academia Brasileira de Ciências 81(1):1–16

Caminos R (1993) El Basamento Metamórfico Proterozoico-Paleozoico inferior. In: Ramos VA (ed) Geología y Recursos Naturales de Mendoza. XII Congreso Geológico Argentino and II Congreso de Exploración de Hidrocarburos, Buenos Aires, pp 11–19

Casquet C, Pankhurst RJ, Fanning CM, Baldo E, Galindo C, Rapela CW, González-Casado JM, Dahlquist JA (2006) U-Pb SHRIMP zircon dating of Grenvillian metamorphism in Western Sierras Pampeanas (Argentina): correlation with the Arequipa-Antofalla craton and constraints on the extent of the Precordillera terrane. Gondwana Res 9:524–529

Cingolani CA, Varela R (1999) The San Rafael Block, Mendoza (Argentina): Rb-Sr isotopic age of basement rocks. II South American Symposium on Isotope Geology, Anales 34 SEGEMAR, Actas 23–26. Carlos Paz, Córdoba

Cingolani CA, Llambías EJ, Ortiz LR (2000) Magmatismo básico pre-Carbónico de El Nihuil, Bloque de San Rafael, Provincia de Mendoza, Argentina. 9° Congreso Geológico Chileno 2:717–721, Puerto Varas

Cingolani CA, Llambías EJ, Basei MAS, Varela R, Chemale Jr F, Abre P (2005) Grenvillian and Famatinian-age igneous events in the San Rafael Block, Mendoza Province, Argentina: geochemical and isotopic constraints. Gondwana 12 conference, Abstracts 102, Mendoza

Cingolani CA, Basei MAS, Uriz NJ, Manassero MJ (2012a) Las metasedimentitas del Paleozoico Medio en el subsuelo de Mendoza (Corral de Lorca): su importancia en la evolución tectónica del Terreno Cuyania. XV Reunión de Tectónica. San Juan, Argentina. Octubre 2012, pp 38–39

Cingolani C, Uriz N, Marques J, Pimentel M (2012b) The Mesoproterozoic U-Pb (LA-ICP-MS) age of the Loma Alta Gneissic rocks: basement remnant of the San Rafael Block, Cuyania Terrane, Argentina. In: Proceedings of 8° South American Symposium on Isotope Geology. CD-ROM version. Medellín, Colombia. Abstract, p 140

Cingolani CA, Uriz NJ, Manassero M, Basei MAS (2014) La Formación Cerro Las Pacas al sur del Cerro Nevado, Mendoza: ¿Basamento Precámbrico o parte de la cuenca devónica de San Rafael? XIX Congreso Geológico Argentino. Córdoba. Argentina. Acta CD-ROM. Resumen: Tectónica Preandina, S21-11

Cingolani CA, Llambías EJ, Chemale Jr F, Abre P, Uriz NJ (this volume) Lower Paleozoic 'El Nihuil Dolerites': Geochemical and isotopic constraints of mafic magmatism in an extensional setting of the San Rafael Block, Mendoza, Argentina. In: Cingolani C (ed) Pre-Carboniferous evolution of the San Rafael Block, Argentina. Implications in the SW Gondwana margin. Springer, Berlin

Criado Roqué P (1972) Bloque de San Rafael. In: Leanza AF (ed) Geología Regional Argentina. Academia Nacional de Ciencias, Córdoba, pp 283–295

Criado Roqué P (1979) Subcuenca de Alvear. Segundo Simposio de Geología Regional Argentina v1. Academia Nacional de Ciencias, Córdoba, pp 811–836

Criado Roqué P, Ibáñez G (1979) Provincia geológica Sanrafaelino-Pampeana. Geología Regional Argentina, Academia Nacional de Ciencias de Córdoba 1:837–869

Dalla Salda L, Cingolani C, Varela R (1992) Early Paleozoic orogenic belt of the Andes in southwestern South America: result of Laurentia-Gondwana collision? Geology 20:617–620

Davicino RE, Sabalúa JC (1990) El Cuerpo Básico de El Nihuil, Dto. San Rafael, Pcia. de Mendoza, Rep. Argentina. 11° Congreso Geológico Argentino, Actas I, 43–47. San Juan

DePaolo DJ (1981) Neodymium isotopes in the Colorado Front Range and crust-mantle evolution in the Proterozoic. Nature 291:193–196

Dessanti RN (1956) Descripción geológica de la Hoja 27c-cerro Diamante (Provincia de Mendoza). Dirección Nacional de Geología y Minería. Boletín 85, 79 p. Buenos Aires

Drummond MS, Defant MJ (1990) A model for trondhjemite-tonalite-dacite genesis and crustal growth via slab melting: Archean to modern comparisons. Journal of Geophysical Research 95 (B13):21503–21521

Faure G (1986) Principles of isotope geology, 2nd edn. Wiley, New York

Hamilton PJ, O'Nions RK, Bridgwater D, Nutman A (1983) Sm-Nd studies of Archaean metasediments and metavolcanics from West Greenland and their implications for the Earth's early history. Earth Planet Sci Lett 62:263–272

Heredia S (1996) El Ordovícico del Arroyo Ponón Trehué, sur de la provincia de Mendoza. XIII Congreso Geológico Argentino y III Congreso de Exploración de Hidrocarburos, Actas I, 601–605

Heredia S (2006) Revisión estratigráfica de la Formación Ponón Trehué (Ordovícico), Bloque de San Rafael, Mendoza. INSUGEO, Serie Correlación Geológica 21:59–74

Heredia S, Mestre A (this volume) Ordovician conodont biostratigraphy of the Ponón Trehué Formation, San Rafael Block, Mendoza, Argentina. In: Cingolani C (ed) Pre-Carboniferous evolution of the San Rafael Block, Argentina. Implications in the SW Gondwana margin. Springer, Berlin

Holmberg E (1973) Descripción Geológica de la Hoja 29d, Cerro Nevado. Servicio Geológico Minero Argentino (SEGEMAR), Boletín 144. Buenos Aires, p 71

Keller M (1999). Argentine Precordillera. Sedimentary and plate tectonic history of a Laurentian crustal fragment in South America. The Geological Society of America, Special Paper 341, pp 1–131

Krogh TE (1973) A low-contamination method for hydrothermal decomposition of Zircon an extraction of U and Pb for isotopic age determinations. Geochemica et Cosmochimica Acta 37 (3):485–494

Kumar A, Heaman LH, Manikyamba C (2007) Mesoproterozoic kimberlites in south India: a possible link to ~1.1 Ga global magmatism. Precambrian Res 154:192–204

Ludwig KR (1999) Using Isoplot/Ex, version 2. A geochronological toolkit for Microsoft excel. Berkeley Geochronological Center, Special Publication 1a, 47 p

Ludwig KR (2001) Squid 1.02: a user manual. Berkeley Geochronology Center, Special Publication, 2, 19 p

Ludwig KR (2003) Isoplot/EX version 3.0, A geochronological toolkit for Microsoft Excel: Berkeley Geochronology Center Special Publication

Ludwig KR (2012) A geochronological toolkit for Microsoft Excel, version 3.76. Berkeley Geochronology Center, Special Publication No 5, Berkeley, 75 p

Morata D, Castro de Machuca B, Arancibia G, Pontoriero S, Fanning CM (2010) Peraluminous Grenvillian TTG in the Sierra de Pie de Palo, Western Sierras Pampeanas, Argentina: petrology, geochronology, geochemistry and petrogenetic implications. Precambr Res 177 (2010):208–322

Nuñez E (1962) Sobre la presencia del Paleozoico inferior fosilífero en el Bloque de San Rafael. Primeras Jornadas Geológicas Argentinas, II:185–189. Buenos Aires

Nuñez E (1976) Descripción geológica de la Hoja 28-C "Nihuil", Provincia de Mendoza. Servicio Geológico Nacional. Buenos Aires (unpublished report)

Nuñez E (1979) Descripción geológica de la Hoja 28d, Estación Soitué, Provincia de Mendoza. Servicio Geológico Nacional, Boletín 166:1–67

Padula E (1949) Descripción geológica de la Hoja 28-C "El Nihuil", Provincia de Mendoza. YPF (unpublished report)

Padula E (1951) Contribución al conocimiento geológico del ambiente de la Cordillera Frontal, Sierra Pintada, San Rafael (Mendoza). Revista de la Asociación Geológica Argentina 6(1):5–13. Buenos Aires

Polanski J (1949) El bloque de San Rafael. Dirección de Minas de Mendoza (unpublished report), Mendoza

Ramos VA (1995) Sudamérica: Un mosaico de continentes y océanos. Ciencia Hoy 6(32):24–29. Buenos Aires

Ramos VA, Dallmeyer RD, Vujovich G (1999) Time constraints on the Early Palaeozoic docking of the Precordillera, central Argentina. In Pankhurst RJ, Rapela CW (eds) The Proto–Andean Margin of Gondwana. Geological Society, Special Publications, 142, London, pp 143–158

Ramos VA (2004) Cuyania, an exotic block to Gondwana: review of a historical success and the present problems. Gondwana Res 7:1009–1026

Ramos VA, Jordan T, Allmendinger R, Mpodozis C, Kay S, Cortés J, Palma M (1986) Paleozoic terranes of the central Argentine-Chilean Andes. Tectonics 5:855–888

Ramos VA, Dallmeyer R, Vujovich GI (1998) Time constrains on the Early Paleozoic docking of the Precordillera central Argentina. In: Pankhurst RJ, Rapela CW (eds) The Proto-Andean margin of Gondwana. Geological Society of London, Special Publication, 142, pp 143–158

Rapela CW, Pankhurst RJ, Casquet C, Baldo E, Galindo C, Fanning CM, Dahlquist JM (2010) The Western Sierras Pampeanas: protracted Grenville-age history (1330–1030 Ma) of intra-oceanic arcs, subduction-accretion at continental edge and AMCG intraplate magmatism. J South Am Earth Sci 29:105–127

Rapp RP, Shimizu N, Norman MD, Applegate GS (1999) Reaction between slab-derived melts and peridotite in the mantle wedge: experimental constraints at 3.8 GPa. Chem Geol 160:335–356

Rolleri EO, Criado Roqué P (1970) Geología de la Provincia de Mendoza. IV Jornadas Geológicas Argentinas (Mendoza, 1969), II:1–60. Buenos Aires

Rolleri EO, Fernández Garrasino CA (1979) Comarca septentrional de Mendoza. Segundo Simposio de Geología Regional Argentina, vol 1. Academia Nacional de Ciencias, Córdoba, pp 771–800

Sato AM, Tickyj H, Llambías EJ, Sato K (2000) The Las Matras tonalitic-trondhjemitic pluton, central Argentina: Grenvillian-age constraints, geochemical characteristics, and regional implications. J S Am Earth Sci 13:587–610

Sato AM, Tickyj H, Llambías EJ, Basei MAS, González PD (2004) Las Matras Block, Central Argentina (37°S-67°W): the Southernmost Cuyania Terrane and its Relationship with the Famatinian Orogeny. Gondwana Res 7(4):1077–1087

Sato K, Kawashita K (2002) Espectrometria de massas em Geologia Isotopica. Revista do Instituto de Geociencias-USP. Geol. USP Serie Científica, Sao Paulo 2:57–77

Sato K, Siga Jr O, Silva JA, McReath I, Liu D, Iizuka T, Rino S, Hirata T, Sproesser WM, Basei MAS (2009) In situ isotopic analyses of U and Pb in Zircon by remotely operated SHRIMP II, and Hf by LA-ICP-MS: an example of dating and genetic evolution of Zircon by $^{176}Hf/^{177}Hf$ from the Ita Quarry in the Atuba Complex, SE Brazil. Geol USP, Série Cientifica São Paulo 9:61–69

Stappenbeck R (1913) Apuntes hidrogeológicos sobre el sudeste de la Provincia de Mendoza. Bol. 6 (Serie B). Dirección General de Minas, Buenos Aires

Stacey JS, Kramers JD (1975) Approximation of terrestrial lead isotope evolution via two-stage model. Earth Planet Sci Lett 26:207–221

Steiger RH, Jager E (1977) Subcommission on geochronology: convention on the use of decay constants in geochronology and cosmochronology. Contrib Geol Time Scale, AAPG Stud Geol 6:67–71

Tanimizu M, Ishikawa T (2006) Development of rapid and precise Pb isotope analytical techniques using MC-ICP-MS and new results for GSJ rock reference samples. Geochem J 40:121–133

Taylor SR, McLennan SM (1985) The continental crust: its composition and evolution. Blackwell, Oxford, 312 p

Thomas WA, Tucker RD, Astini RA, Denison RE (2012) Ages of pre-rift basement and synrift rocks along the conjugate rift and transform margins of the Argentine Precordillera and Laurentia. Geosphere 8(6):1366–1383

Varela R, Basei MAS, González PD, Sato AM, Naipauer M, Campos Neto M, Cingolani CA, Meira VT (2011) Accretion of Grenvillian terranes to the southwestern border of the Río de la Plata craton, western Argentina. Int J Earth Sci 100:243–272

Vujovich GI, Van Staal CR, Davis W (2004) Age constraints on the tectonic evolution and provenance of the Pie de Palo complex, Cuyania composite terrane, and the Famatinian Orogeny in the Sierra de Pie de Palo, San Juan, Argentina. Gondwana Res 7(4):1041–1056

Wichmann R (1928) Reconocimiento geológico de la región de El Nihuil, especialmente relacionado con el proyectado dique de embalse del Río Atuel. Dirección Nacional de Minería (unpublished report). Buenos Aires

Williamson JH (1968) Least-squares fitting of a straight line. Can J Phys 46:1845–1847